Phylogenetics of the mycoheterotrophic genus Thismia (Thismiaceae: Dioscoreales) with a focus on the Old World taxa: delineation of novel natural groups and insights into the evolution of morphological traits

Ekaterina A Shepeleva , Mikhail I Schelkunov , Michal Hroneš , Michal Sochor , Martin Dančák , Vincent Sft Merckx , Izai Abs Kikuchi , Sahut Chantanaorrapint , Kenji Suetsugu , Hirokazu Tsukaya , Shek S Mar , Hong Truong Luu , Hong-Qing Li , Maria D Logacheva , Maxim S Nuraliev

Botanical Journal of the Linnean Society, 2020, **193**, 287–315. With 7 figures.

Phylogenetics of the mycoheterotrophic genus *Thismia* (Thismiaceae: Dioscoreales) with a focus on the Old World taxa: delineation of novel natural groups and insights into the evolution of morphological traits

EKATERINA A. SHEPELEVA[1], MIKHAIL I. SCHELKUNOV[2,3], MICHAL HRONEŠ[4], MICHAL SOCHOR[5], MARTIN DANČÁK[4], VINCENT S.F.T. MERCKX[6], IZAI A.B.S. KIKUCHI[6,7], SAHUT CHANTANAORRAPINT[8], KENJI SUETSUGU[9], HIROKAZU TSUKAYA[10], SHEK S. MAR[11], HONG TRUONG LUU[12], HONG-QING LI[13], MARIA D. LOGACHEVA[1,2,3] and MAXIM S. NURALIEV[1,14,*]

[1]*M.V. Lomonosov Moscow State University, 119234 Moscow, Russia*
[2]*Skolkovo Institute of Science and Technology, 143025 Moscow, Russia*
[3]*Institute for Information Transmission Problems, 101447 Moscow, Russia*
[4]*Faculty of Science, Palacký University, CZ-77146 Olomouc, Czech Republic*
[5]*Centre of the Region Haná for Biotechnological and Agricultural Research, Crop Research Institute, Šlechtitelů 29, Olomouc, CZ-78371, Czech Republic*
[6]*Naturalis Biodiversity Center, P.O. Box 9517, 2300 RA Leiden, The Netherlands*
[7]*Leiden University, Hortus botanicus, 5e Binnenvestgracht 8, 2311 VH Leiden, The Netherlands*
[8]*Department of Biology, Faculty of Science, Prince of Songkla University, Hat Yai, Songkhla 90112, Thailand*
[9]*Department of Biology, Graduate School of Science, Kobe University, 1-1 Rokkodai, Nada-ku, Kobe, 657–8501, Japan*
[10]*Department of Biological Sciences, Graduate School of Science, The University of Tokyo, 7-3-1 Hongo, Bunkyo-ku, Tokyo 13–0033, Japan*
[11]*Ying Wa College, Hong Kong*
[12]*Southern Institute of Ecology & Graduate University of Science and Technology, Vietnam Academy of Science and Technology, 1A, TL29 Street, Thanh Loc Ward, District 12, Ho Chi Minh City, Vietnam*
[13]*School of Life Sciences, East China Normal University, 500 Dongchuan Road, Shanghai, 200241, China*
[14]*Joint Russian-Vietnamese Tropical Scientific and Technological Center, Hanoi, Vietnam*

Received 26 July 2019; revised 4 November 2019; accepted for publication 16 February 2020

Thismia is a genus of > 80 mycoheterotrophic species characterized by a peculiar appearance and complex floral morphology. A significant proportion of the species and morphological diversity of *Thismia* has only been uncovered in the past two decades, and new discoveries continue to be made. Given that many new data have recently become available, and the most comprehensive taxonomic revision of the genus from 1938 addresses less than half of the currently known species, previous hypotheses for species relationships and infrageneric taxonomic classification in *Thismia* was in need of review. Extensive molecular phylogenetic studies of *Thismia* at the genus level have never been presented. We investigate the phylogenetic relationships of 41 species (and one variety) of *Thismia* from the Old World. Our study comprises 68 specimens (for 28 of which the data were newly generated), including outgroup taxa broadly representing Thismiaceae (= Burmanniaceae *p.p. sensu* APG IV, 2016), and is based on two nuclear and one mitochondrial marker. We use maximum likelihood and Bayesian inference to infer relationships among

*Corresponding author. E-mail: max.nuraliev@gmail.com

the taxa. We also constructed a morphological dataset of 12 mostly floral characters, comparing these characters to hypotheses based on molecular evidence to identify putative synapomorphies for major clades and to discuss hypotheses regarding the evolution of structural traits in the genus. Our analyses indicate that the majority of currently accepted infrageneric taxa of *Thismia* are polyphyletic. We find support for the monophyly of the Old World group, in which we recognize five well-supported lineages (clades); the only New World species studied appears to be related to the Neotropical genus *Tiputinia*. Ancestral state reconstructions demonstrate that the evolution of most morphological characters was homoplastic, but we identify characters that provide each of the five clades of Old World *Thismia* with a unique morphological description. The geographical distribution of the species under study is also shown to be consistent with the major clades. Our investigation provides a phylogenetic basis for the development of a novel sectional classification of *Thismia* reflecting morphological and geographical traits.

KEYWORDS: floral traits – high-throughput sequencing – molecular phylogenetics – monocots – non-photosynthetic plants – South-East Asia.

INTRODUCTION

Thismia Griff. (Thismiaceae) (Griffith, 1845), commonly known as the fairy lanterns, is a genus of fully mycoheterotrophic, non-photosynthetic herbs with a disjunct distribution range split between tropical and subtropical Asia to temperate Australia and (mostly) tropical America (Maas-Van de Kamer, 1998; Merckx *et al.*, 2013; Merckx & Smets, 2014). The highest species diversity of *Thismia* is found in Borneo and the Malay Peninsula (Chantanaorrapint, 2012; Tsukaya & Okada, 2012; Sochor, Hroneš & Dančák, 2018b). *Thismia* spp. are remarkable for their peculiar appearance and the morphology of the flowers, which are distinctive and at the same time quite diverse (Fig. 1). Above the inferior ovary, there is a prominent hypanthium (also called a flower tube or flower chamber) that bears six tepals and six stamens. The stamens hang down inside the hypanthium and thus are invisible from the outside. The anthers usually fuse postgenitally with each other into a tube by their connectives and possess various hairs and appendages. The three outer tepals are always free (or absent), whereas the inner tepals are sometimes fused into a roof-like or hat-like structure called a mitre (Fig. 1B–H). One or both whorls of tepals often bear filiform or cylindrical appendages (Fig. 1A, C, D, F, I–L) (Maas-Van de Kamer, 1998; Merckx *et al.*, 2013; Merckx & Smets, 2014).

A member of Dioscoreales, *Thismia* is currently placed by many researchers in Thismiaceae (Stevens, 2001; Merckx *et al.*, 2013, 2017; Lam *et al.*, 2018; Sochor *et al.*, 2018b). However, phylogenetic relationships in Dioscoreales are still largely unresolved at the family level and, consequently, delimitation of the order into families remains unstable (e.g. Kumar *et al.*, 2017; Chantanaorrapint & Suddee, 2018). In the APG system (APG III, 2009; APG IV, 2016), a broad understanding of families of Dioscoreales was provisionally accepted, with Thismiaceae included in Burmanniaceae and Taccaceae in Dioscoreaceae (but see Lam, Merckx & Graham, 2016). However, further studies are needed to resolve existing incongruences: some molecular phylogenetic studies have shown that representatives of Thismiaceae are rather distantly related to Burmanniaceae *s.s.*, which led to consideration of the former as a separate family (Merckx *et al.*, 2006, 2009; Merckx, Huysmans & Smets, 2010; Lam *et al.*, 2016, 2018), whereas other molecular phylogenetic reconstructions recover Thismiaceae as paraphyletic with respect to *Tacca* J.R.Forst. & G.Forst., traditionally accepted as the only genus of Taccaceae (Merckx & Bidartondo, 2008; Merckx *et al.*, 2009, 2010; Merckx & Smets, 2014). The precise topology differs considerably depending on the DNA regions and methods of reconstruction (Merckx *et al.*, 2009). Here, while acknowledging the uncertainty relating to phylogenetic relationships in the group, we choose to recognize Thismiaceae as a separate family.

To maintain Thismiaceae and make it monophyletic, Hunt, Steenbeeke & Merckx (2014) suggested excluding *Afrothismia* Schltr. However, appropriate taxonomic and nomenclatural changes necessary for the family placement of *Afrothismia* have never been published. Thismiaceae, including *Afrothismia*, are subdivided into five genera, of which *Thismia* is by far the largest, comprising almost 80% of the family. So far, > 80 species of *Thismia* have been accepted (Dančák *et al.*, 2018; Sochor *et al.*, 2018a; Suetsugu *et al.*, 2018; Chantanaorrapint *et al.*, 2019; Siti-Munirah & Dome, 2019), and several new species are described each year. The other genera are *Afrothismia* with 16 species, *Oxygyne* Schltr. with six species and the monotypic *Tiputinia* P.E.Berry & C.L.Woodw. and *Haplothismia* Airy Shaw (Merckx *et al.*, 2013; Cheek *et al.*, 2018; Cheek, Etuge & Williams, 2019). Similar to the situation at the family level, the monophyly of *Thismia* also represents an open question: according to phylogenetic analyses of molecular and morphological data sets, certain New World *Thismia* spp. do not group with the rest of the genus (Merckx *et al.*, 2006, 2009; Yokoyama *et al.*, 2008; Merckx & Smets, 2014).

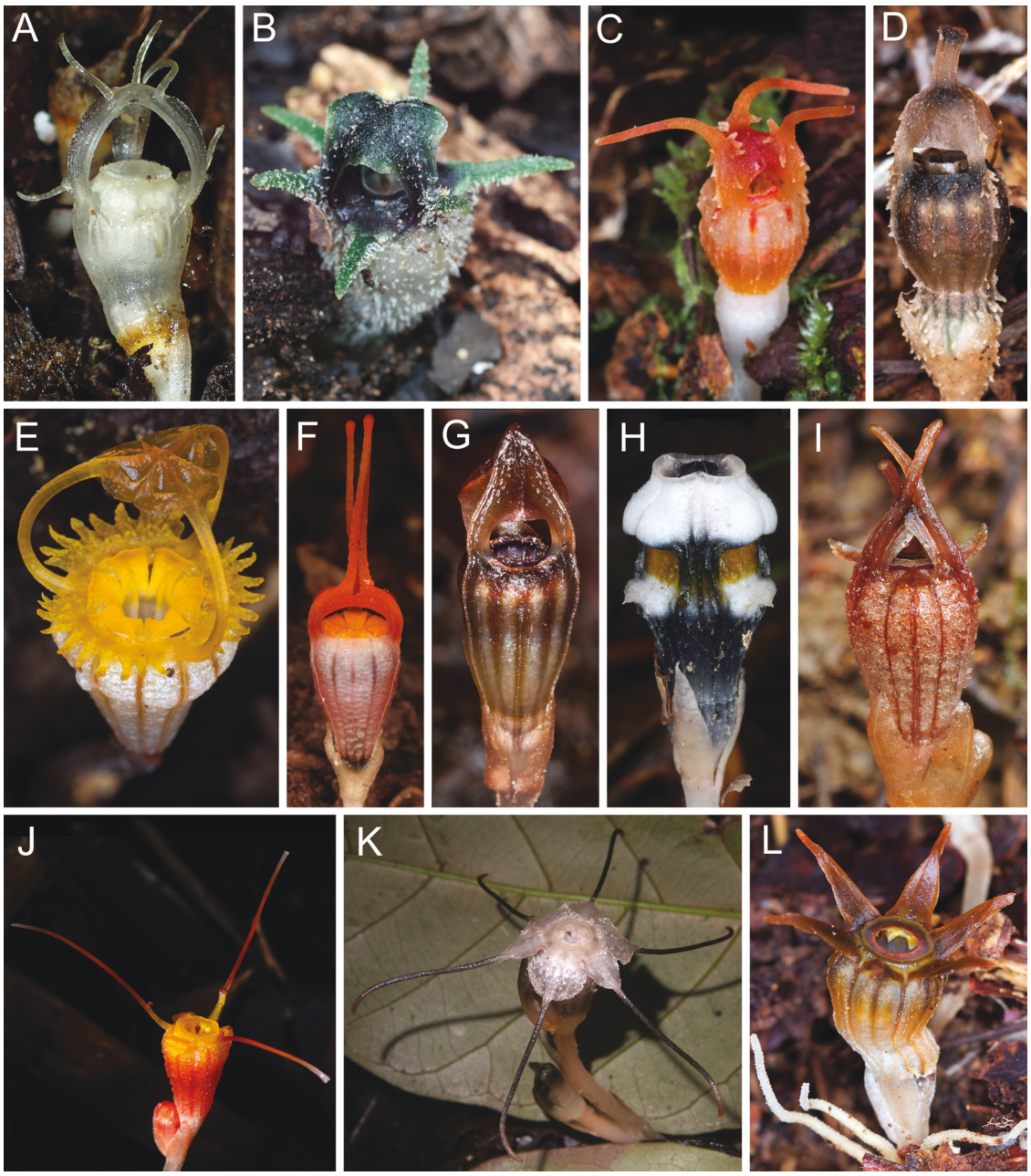

Figure 1. Representative diversity of flowers of Asian *Thismia*. A, *T. abei*. B, *T. thaithongiana*. C, *T. minutissima*. D, *T. viridistriata*. E, *T. kelabitiana*. F, *T. clavigera*. G, *T. acuminata*. H, *T. mirabilis*. I, *T. hongkongensis*. J, *T. gardneriana*. K, *T. annamensis*. L, *T. inconspicua*. Photographs. A, K. Suetsugu; B, F, H, J, S. Chantanaorrapint; C, D, E, G, L, M. Sochor; I, S.S. Mar; K, M.S. Nuraliev.

The most recent taxonomic revision of *Thismia* at a worldwide scale was published by Jonker (1938; see also Jonker, 1948), who presented a detailed classification and introduced a number of sections and subsections. Since then, the number of species currently assigned to *Thismia* has more than doubled, and some of the newly described species show combinations of morphological characters and geographical patterns that do not fit within the infrageneric framework established by Jonker (Thiele & Jordan, 2002; Nuraliev *et al.*, 2014, 2015). The cladistic analysis of morphological features performed by Merckx & Smets (2014) demonstrated that some infrageneric taxa are not monophyletic, which may be consistent with a degree of convergence in the morphological traits used in traditional systems of *Thismia*. To facilitate further phylogenetic

investigations of *Thismia*, Kumar *et al.* (2017) compiled an updated version of the traditional system in which they adopted the modifications suggested by Maas *et al.* (1986) and Merckx & Smets (2014), listing all of the species known at the time of their work. Only some groups of *Thismia*, mainly from Australia and Borneo (Sarawak state of Malaysia and Brunei) and totalling *c*. 20 species, have been studied to date using molecular phylogenetics (Hunt *et al.*, 2014; Merckx & Smets, 2014; Merckx *et al.*, 2017; Kumar *et al.*, 2017; Sochor *et al.*, 2018b). These studies confirm that the current taxonomic system does not reflect actual phylogenetic relationships, and they clearly indicate the necessity for a large-scale reconstruction with inclusion of representatives from all geographical areas and morphological types.

Here, we study the phylogenetics of *Thismia* with a sampling of 42 species and a focus on mainland South-East Asia. We use the results to investigate the evolution of some morphological traits that are traditionally used for circumscription of infrageneric taxa in the genus. This study is a precursor to a comprehensive taxonomic revision of *Thismia* based on the current phylogenetic views and reflecting the biological characteristics of its species.

MATERIAL AND METHODS

Taxon sampling

Data from 42 *Thismia* spp. were used in this study. Nuclear and mitochondrial sequences for 25 species were generated *de novo*, those of 20 species (and one variety) were obtained for the first time. Sequences for a further 22 species were obtained from GenBank. Based on Merckx & Smets (2014) and Hunt *et al.* (2014), 12 representatives of Thismiaceae, Burmanniaceae, Dioscoreaceae and Taccaceae were included as outgroup taxa (Appendix 1).

Molecular techniques and analysis

DNA was extracted from herbarium and silica gel-dried material using the CTAB-based method (Doyle & Doyle, 1987) with the following modifications: chloroform extraction was performed twice. We used three markers: two nuclear markers, the nuclear ribosomal ITS1–2 region (including internal transcribed spacer 1, the 5.8S rRNA gene and internal transcribed spacer 2; together referred to as ITS), a part of the 18S rRNA gene and one mitochondrial region, a part of the *atp1* gene. These regions have previously been successfully used for phylogenetic analysis of mycoheterotrophic plants, including *Thismia* (Merckx *et al.*, 2017). For most of the samples, we used the following PCR primers: 18S-F (TTTGAAGAAATTAGAGTGCTCAAAG) and 18S-R (CTTCCTCTAAATGATAAGGTTCA) for the 18S rRNA gene, *atp1*-F (AAGTGGATGAGATCGGTCGAG) and *atp1*-R (AGTGGCATTCGATCACAGAAGC) for *atp1*, and ITS5 and ITS4 (White *et al.*, 1990; Baldwin, 1992) for the ITS. PCR was performed using Q5 mix (New England Biolabs, USA). The PCR programme consisted of 30 cycles, with each cycle as follows: 10 s at 95 °C, 25 s at 58 °C and 40 s at 72 °C, with an initial denaturation of 1 min 30 s at 95 °C and the final extension for 5 min at 72 °C. Amplicons were run on a 0.8% agarose gel; those samples that produced a clear single band of the expected size were retained for sequencing. Samples were purified using Ampure XP beads (Beckman-Coulter, USA) and sequenced using ABI PRISM BigDye Terminator v.3.1 kit on an Applied Biosystems 3730 DNA Analyser (Thermo Fisher, USA). For the specimens of *T. minutissima* Dančák, Hroneš & Sochor, *T. nigra* Dančák, Hroneš & Sochor, *T. viridistriata* Sochor, Hroneš & Dančák and *T.* sp. Andulau, the primers, PCR programme and conditions of DNA purification and sequencing were selected following Sochor *et al.* (2018b). For the specimens of *T. abei* (Akasawa) Hatus., *T. javanica* J.J.Sm. and *T. kelabitiana* Dančák, Hroneš & Sochor, the following primers were used: NS1 and NS2 (M13 tailed), NS3 and NS4 (M13 tailed), and NS5 and NS8 (without M13 tail) for 18S (White *et al.*, 1990; Oetting *et al.*, 1995), ITS1 and ITS4 (M13 tailed) for ITS (White *et al.*, 1990; Oetting *et al.*, 1995), *atp1*-F-A1 and *atp1*-B-A1 (M13 tailed) for *atp1* (Oetting *et al.*, 1995; Davis *et al.*, 2004). The PCR programme used consisted of 35 cycles, with each cycle as follows: 15 s at 94 °C, 30 s at 44 °C and 40 s at 72 °C, with the initial denaturation for 3 min at 94 °C, and the final extension for 7 min at 72 °C.

For several species for which amplification and/or sequencing of marker regions was unsuccessful, we employed the approach of genome skimming, i.e. low-coverage genome sequencing (Straub *et al.*, 2012). This approach has also been successfully used to recover single-gene data from plastid genomes of Thismiaceae (Lam *et al.*, 2016). This was performed using preparation of shotgun genomic libraries and sequencing on an Illumina platform.

DNA was fragmented using a Covaris S220 sonicator (Covaris, USA) with the following settings: peak power 230, duty cycle 10%, with 200 cycles per burst. These parameters enable fragmentation to the length optimal for library preparation (200–400 bp). Fragmented DNA was prepared for sequencing using a NEBNext Ultra II DNADNA Library Prep Kit for Illumina kit (New England Biolabs, USA). Indexing was performed using NEBNext Multiplex Oligos for Illumina (Index Primers Set 1 for *T. okhaensis* Luu, Tich, G.Tran & Đinh, Index Primers Set 2 for *T. annamensis* K.Larsen & Aver., *T. hexagona*

Dančák, Hroneš, Kobrlová & Sochor and *T. mucronata* Nuraliev). Sequencing was performed on MiSeq for *T. mucronata* using v.2 chemistry and read length equal to 255, in paired-end mode and on HiSeq 2500 for other species using v.4 chemistry and read length equal to 125, in paired-end mode. Demultiplexing was performed using CASAVA-1.8.2 (Illumina) for MiSeq data and bcl2fastq v.2.17.1.14 (Illumina) for HiSeq2500 data. Reads were then trimmed using CLC Genomics Workbench v.9.5.4 and assembled using the same program with the following parameters: word size and bubble size = default, minimal contig length = 1000, mismatch cost = 2, insertion cost = 3, deletion cost = 3, length fraction = 0.98 and similarity fraction = 0.99. Contigs containing *atp1*, 18S and ITS were selected based on a BLAST search using *Thismia* sequences available in GenBank as a query (e-value threshold 10^{-10}, BLASTN v.2.2.10). All sequences that were found as a result of this search were searched back against NCBI nr database, to identify and exclude contaminating sequences.

Multiple sequence alignments were made for the three phylogenetic markers separately. The alignments were performed using the online version of MAFFT 7 (Katoh & Standley, 2013) with all parameters set to the default values, except for the parameter 'Adjust direction according to the first sequence', which was switched on, allowing for sequences to be aligned in the proper direction in case they were reverse complemented in the input FASTA file. Poorly aligned columns were removed by the online version of Gblocks v.0.91b (Castresana, 2000) with the default parameters, except for the 'Allow gap positions within the final blocks' and 'Allow less strict flanking positions', which were switched on to make Gblocks less severe in determining which columns were aligned poorly. The alignments were then concatenated by the script geneStitcher.py from https://github.com/ballesterus/Utensils. In cases where some of the markers were not sequenced for a specimen, corresponding places in the concatenated alignment were filled with gap symbols. The percent of variable sites in the alignments was calculated by AMAS (Borowiec, 2016). The multiple sequence alignments (before and after pruning by GBLOCKS) are available at https://doi.org/10.6084/m9.figshare.8864936.

Phylogenetic reconstructions were performed for the concatenated alignments of the three markers (ITS+18S+*atp1*), for the concatenated alignments of ITS+18S, for the concatenated alignments of 18S+*atp1* and for the alignments of the three markers separately. For the concatenated alignments, the optimal partitioning for the phylogenetic reconstruction was estimated by the program PartitionFinder 2.1.1 (Lanfear *et al.*, 2017) under the GTR+Gamma evolution model, where possible partitions corresponded to individual markers. The best partitioning was selected by the corrected Akaike information criterion (AICc). In all cases, the best partition was the one where all markers were treated separately.

The maximum likelihood (ML) phylogenetic reconstruction was performed by RAxML v.8.2.4 (Stamatakis, 2014), using 20 starting maximum-parsimony trees. The number of bootstrap pseudoreplicates for the bootstrap analysis was selected by RAxML automatically using the majority-rule consensus tree criterion ('autoMRE'). Substitution rates for the partitions were linked. Linking the substitution rates of partitions allows to estimate branch lengths even for samples that lack sequences of some markers.

The Bayesian phylogenetic reconstruction was performed by MrBayes v.3.2.7 (Ronquist *et al.*, 2012) under the GTR+Gamma model of sequence evolution, with four Markov chains, each of 2 500 000 generations, and sampling frequency of 500 generations. Substitution rates for the partitions were linked. Majority-rule consensus trees were calculated after excluding the first 25% of samples. Effective sample sizes were evaluated using Tracer v.1.7.1 (Rambaut *et al.*, 2018). The effective sample sizes were > 200 for all statistics in all datasets, suggesting that the run length was adequate.

Maximum-parsimony phylogenetic reconstruction was not performed because the method of maximum parsimony has been shown to result in inadequate reconstructions for mycoheterotrophic plants (e.g. Lam *et al.*, 2018). Particularly, the sensitivity of parsimony analysis in Thismiaceae to long-branch attraction artefacts using the markers employed here was demonstrated by Merckx *et al.* (2009). ML-based analyses can also be affected by the long-branch attraction, but to a lesser extent (Swofford *et al.*, 2001).

The use of markers from different genomes in combination for phylogenetic reconstruction may be inappropriate because such markers may have different phylogenetic histories (Rubinoff & Holland, 2005). However, a comparison of ML and Bayesian trees built by the nuclear markers (ITS+18S) and the mitochondrial marker (*atp1*) showed that there are no bipartitions significantly (bootstrap support at least 80% or posterior probability at least 95%) different for these two types of markers. Therefore, the combined analyses of the nuclear and mitochondrial markers are justified. The trees were drawn by TreeGraph v.2.14.0-771 beta (Stöver & Müller, 2010).

RECONSTRUCTION OF MORPHOLOGICAL EVOLUTION

To explore morphological evolution, the significance of morphological characters in diagnosing the natural

groups obtained here and the ancestral character states, we created and matched a species-level morphological data matrix (Appendix 2) for species present in the molecular phylogenetic analyses. The morphological data were taken from the species protologues and from the specimens cited in Appendix 1.

Most of the characters and their states (Appendix 3) have been taken from the taxonomic literature. Character scoring was performed according to Brazeau (2011) and generally followed the cladistic analysis of morphological data set by Merckx & Smets (2014). In contrast to Merckx & Smets (2014), we treated the diversity of underground parts as a single character with seven conditions to avoid mixing the cases that are similar in appearance but morphologically different, such as tubers and tuberous roots. For the structure of the inner perianth whorl, we assigned three conditions instead of the two commonly used: tepals free; tepals fused into a mitre (irrespective of tepal aestivation); and tepals overlap forming a loose dome (without fusion). We did not make a distinction between the appendages of free inner tepals and those of a mitre (including dorsal appendages or those arising from a central point); instead, we treated these features as a single character, i.e. absence or presence of appendages of inner tepals. We also specified the conditions of this character and grouped minute appendage-like protuberances (< 1.5 mm long), e.g. in *T. brunneomitra* Hroneš, Kobrlová & Dančák and *T. mucronata*, together with the absence of appendages. Finally, for the stamen number, we assigned both taxa characterized by three stamens in a flower (*Burmannia* L. and *Oxygyne*) with the same condition of this character, because in both genera the stamens represent the inner whorl of the androecium. Although the stamens of *Oxygyne* have been stated by some authors (e.g. Cheek *et al.*, 2018) to be arranged opposite the outer tepals, we have observed that in fact they alternate with the stigmas, which means that the stamens are arranged opposite the inner whorl of tepals.

ML ancestral reconstruction analyses were performed in Mesquite v.3.51 (Maddison & Maddison, 2006, 2018), employing the Markov k-state 1 (Mk1) parameter model of morphological character evolution. The Bayesian majority-rule tree based on the ITS+18S+*atp1* combined dataset was used for the ancestral state reconstructions. Additionally, only one terminal per species was retained, transforming the specimen tree into a putative species tree. Specimens that were not decidedly identified to the species level were discarded from the analysis. The trees with ancestral state reconstructions were drawn by Mesquite. As well as the Mk1 model, we also tested the AsymmMk model. For each binary character, we compared these two models by the likelihood ratio test. Prior to a multiple hypothesis testing correction, there were two characters for which the AsymmMk model was significantly (P value < 0.05) better than the Mk1 model, namely, the characters 'Transverse bars inside the hypanthium' and 'Foveae on mitre surface'. However, after the Benjamini–Hochberg correction for multiple testing all differences became non-significant (q value ≥ 0.05).

RESULTS

Sequencing

Using Sanger sequencing we obtained the sequences for all three markers for 17 *Thismia* spp., and we obtained the sequences for either one or two markers for eight additional species. In addition, we analysed genome skimming data for four specimens. For three samples, Sanger sequencing was unsuccessful for all three markers: *T. annamensis* (*Averyanov et al. HLF 5510*, the type specimen), *T. hexagona* (*Hroneš s.n.*) and *T. okhaensis*. For *T. mucronata*, the type specimen (*Nuraliev 813*) was studied using a genome skimming approach, whereas the other specimen (*Nuraliev 1009*) was studied using Sanger sequencing. Sequences of *Thismia tentaculata* K.Larsen & Aver. were assembled from the sample for which complete plastome structure was reported earlier (Lim *et al.*, 2016). Using raw reads from their study, we assembled high copy regions and extracted *atp1*, 18S and ITS sequences. The results of the BLAST search that were used to identify marker regions in the contigs indicated the presence of contaminating sequences in the samples of *T. hexagona* and *T. okhaensis*. The examination of BLAST results allowed to identify possible source of contamination (see also Supporting Information, Supplementary Table 1).

Phylogenetic analysis

The main characteristics of the alignments are listed in Table 1. The ML and Bayesian approaches for the combined dataset resulted in congruent tree topologies (Figs 2, 3). Among the analyses of separate markers (Supporting Information, Supplementary Figs 1–6), those based on the 18S gene (Supporting Information, Supplementary Figs 3, 4) were most congruent with the three-marker trees and showed lower support for some clades, including some small clades within the five major clades (see below) and the relationships between the major clades; the analyses based on the *atp1* gene (Supporting Information, Supplementary Figs 5, 6) resulted in trees generally similar to the three-marker trees with a number of differences in topology, such as different relationships between the

Table 1. Multiple alignment statistics.

Marker	Alignment length (bp)	Alignment length after pruning by Gblocks (bp)	Number of variable sites in the alignment after pruning by Gblocks (bp)	Percent of variable sites in the alignment after pruning by Gblocks
ITS	1597	321	233	67%
18S rDNA	2827	1712	405	23.7%
atp1	1571	1265	239	18.9%

major clades and different position of several species (*T. gardneriana* Hook.f. ex Thwaites, *T. mucronata*, *T. nigricans* Chantanaorr. & Sridith, *T. viridistriata*); the analyses based on the ITS region (Supporting Information, Supplementary Figs 1, 2) were the most different, especially in the position of the major clades and the species *T. hongkongensis* Mar & R.M.K.Saunders and *T. panamensis* (Standl.) Jonker, although they still supported most of the major clades.

In the trees based on the combined dataset, *T. panamensis*, the only New World species of *Thismia* included in the analysis, grouped together with the monotypic Neotropical *Tiputinia*. The others formed a well-supported clade referred to here as the Old World clade [posterior probability (PP) 1.00, bootstrap percentage in the maximum likelihood analysis (BP_{ML}) 100]. Five well-supported major clades were identified in the Old World clade. Clade 1 (PP 1.00, BP_{ML} 100) comprised six species, three of which inhabit mainland East and South-East Asia (*T. gongshanensis* Hong Qing Li & Y.K.Bi, *T. nigricoronata* Kumar & S.W.Gale, *T. thaithongiana* Chantanaorr. & Suddee) and three others inhabit the islands of East Asia (*T. abei*, *T. huangii* P.Y.Jiang & T.H.Hsieh, *T. taiwanensis* Sheng Z.Yang, R.M.K.Saunders & C.J.Hsu). Clade 2 (PP 1.00, BP_{ML} 100) consisted of four species from south-eastern Australia and New Zealand [*T. clavarioides* K.R.Thiele, *T. hillii* (Cheeseman) N.Pfeiff., *T. megalongensis* C.A.Hunt, G.Steenbee. & V.Merckx, *T. rodwayi* F.Muell.] and '*Thismia* sp.', a taxon from New South Wales of uncertain taxonomic status. Clade 3 (PP 0.95, BP_{ML} 97) comprised seven Bornean species (*T. acuminata* Hroneš, Dančák & Sochor, *T. betung-kerihunensis* Tsukaya & H.Okada, *T. brunneomitra*, *T. clavigera* F.Muell., *T. kelabitiana*, *T. laevis* Sochor, Dančák & Hroneš, *T. nigra*); *T. clavigera* also occurs in Peninsular Thailand and Sumatra (but see Suetsugu *et al.*, 2018). Clade 4 (PP 1.00, BP_{ML} 99) included six species from Vietnam and Thailand (*T. angustimitra* Chantanaorr., *T. mirabilis* K.Larsen, *T. mucronata*, *T. nigricans*, *T. okhaensis*, *T. puberula* Nuraliev). Clade 5 (PP 1.00, BP_{ML} 100), the largest clade, comprised ten species, ranging from the Indochinese Peninsula to Borneo (*T. alba* Holttum ex Jonker, *T. annamensis*, *T. aseroe* Becc., *T. bryndonii* Tsukaya, Suetsugu & Suleiman, *T. cornuta* Hroneš, Sochor & Dančák, *T. filiformis* Chantanaorr., *T. hexagona* including var. *grandiflora* Tsukaya, Suleiman & H.Okada, *T. inconspicua* Sochor & Dančák, *T. neptunis* Becc., *T. pallida* Hroneš, Dančák & Rejžek) and '*Thismia* sp. Andulau', a taxon from Brunei of uncertain taxonomic status. In addition, several species occupied rather isolated and unstable positions: these are *T. minutissima*, *T. viridistriata*, *T. hongkongensis*, *T. gardneriana*, *T. tentaculata* and *T. javanica*. Within ML and Bayesian inference, the following topology was recognized as follows: clade 1; clade 2; *T. minutissima*; clade 3 + *T. viridistriata*; clade 4 and the remaining Old World *Thismia* spp.

To check possible infraspecific variability, some species were studied using material from more than one population. Most of these species showed no or few (one or two substitutions) differences between sequences obtained from different accessions, and almost all species represented by more than one accession formed monophyletic groups. The only exception is *T. mucronata*, which showed uncertain relationships with other species of clade 4.

Evolution of morphological characters

A matrix with 12 morphological characters was created. One of them (the number of stamens) is invariable in the Old World clade, whereas the others are mostly homoplastic according to the ML state reconstruction (Figs 4–7; Supplementary trees; Supplementary Mesquite file). Nevertheless, some characters are useful for defining certain natural (monophyletic) groups within the Old World clade. Clade 1 is unique in the absence of interstaminal glands and absence of a wing-like (often called lateral) appendage of a connective; these features are found only in this clade and characterize all of its species. Clade 1 uniformly shows the absence of transverse bars inside the hypanthium. Finally, it is the only clade that comprises species with free stamen connectives (along with species with the connectives fused into a tube). Clade 2 is characterized by the absence of transverse bars inside the hypanthium, the presence of appendages of inner tepals, inner tepals

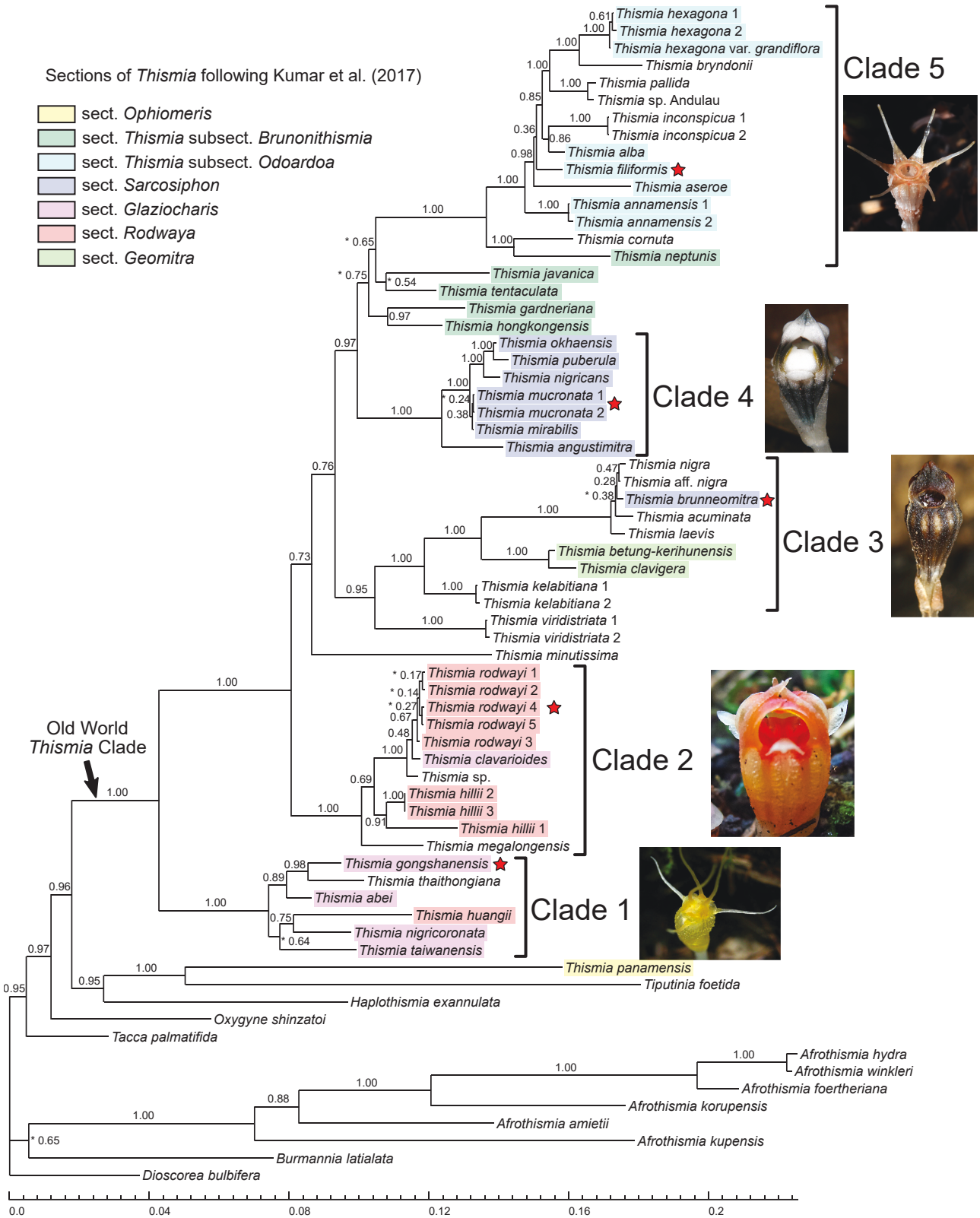

Figure 2. Bayesian tree obtained from the analysis of the combined ITS+18S+*atp1* dataset. Numbers near branches are posterior probabilities (PP); asterisks in front of these numbers indicate the clades that are not supported by ML analysis (Fig. 3). The representatives of clades 1–5 illustrated with photographs are indicated by stars. Photographs. *Thismia*

fused into a mitre and the absence of mitre foveae. Clade 3 is characterized by coralliform roots (which represent its synapomorphy and unique feature), inner tepals fused into a mitre, absence of mitre foveae; it comprises the only two species of *Thismia* included in our analysis that show free mitre appendages arising from a central point. Clade 4 is characterized by the absence of transverse bars inside the hypanthium, the absence of appendages of outer and inner tepals and inner tepals fused into a mitre. The presence of mitre foveae is a unique feature of this clade (most likely, a synapomorphy), which occurs in four out of its six species (absent in *T. mucronata* and *T. okhaensis*). Clade 5 is characterized by free inner tepals and the presence of appendages of outer and inner tepals.

DISCUSSION

Phylogenetics and traditional taxonomy of *Thismia*

Our taxonomic sample (42 out of *c*. 80 species known worldwide) covers a significant portion of the morphological variability and geographical range of *Thismia* in the Old World. Additionally, our analyses generally resolved major groups with strong branch support. Thus, our findings will allow for the morphology-based classification systems to be evaluated in a phylogenetic framework and provide insight into patterns of morphological evolution with emphasis on Asian and Australian representatives.

Thismia is currently subdivided into two subgenera, of which *Thismia* subgenus *Thismia* accommodates all of the Old World species plus *T. americana* N.Pfeiff. and subgenus *Ophiomeris* (Miers) Maas & H.Maas comprises all of the Neotropical species (Maas *et al.*, 1986; Merckx & Smets, 2014; Kumar *et al.*, 2017). Similar to recent studies (Merckx *et al.*, 2006, 2009; Yokoyama *et al.*, 2008; Merckx & Smets, 2014), our results suggest that *Thismia* is polyphyletic, with *Thismia* subgenus *Ophiomeris* (represented here by a single species, *T. panamensis*) being only distantly related to subgenus *Thismia*. The Old World clade in our trees corresponds to subgenus *Thismia*, tentatively confirming the monophyly of this taxon.

The subdivisions of *Thismia* subgenus *Thismia* accepted in Kumar *et al.* (2017) appear to be largely polyphyletic according to our molecular phylogenetic reconstructions. Of the six sections of this subgenus, *Thismia* section *Scaphiophora* (Schltr.) Kumar & S.W.Gale comprising two species, is absent from our analysis. Section *Geomitra* (Becc.) Kumar & S.W.Gale, which consists of *T. betung-kerihunensis* and *T. clavigera*, formed a monophyletic group in clade 3. Representatives of *Thismia* sections *Rodwaya* (Schltr.) Jonker and *Glaziocharis* (Taub. ex Warm.) Hatus. are scattered between clades 1 and 2. Transfer of the only Asian species of section *Rodwaya*, *T. huangii*, to section *Glaziocharis* and of the only Australian species of section *Glaziocharis*, *T. clavarioides*, to section *Rodwaya*, would make section *Glaziocharis* and section *Rodwaya* fully conform with clades 1 and 2. This modification of sectional taxonomy would also be in agreement with several morphological traits (presence of stamen appendages and presence of interstaminal glands). The species of the large *Thismia* section *Sarcosiphon* (Blume) Jonker are mainly placed in clade 4, but we also recovered at least one in clade 3. The type section, *Thismia* section *Thismia* is further subdivided into two subsections. Clade 5 corresponds to section *Thismia* subsection *Odoardoa* Schlechter (except for inclusion in the clade of *T. neptunis*, classified in section *Thismia* subsection *Brunonithismia* Jonker); most of the other species of subsection *Brunonithismia* (i.e. *T. gardneriana*, *T. hongkongensis*, *T. javanica*, *T. tentaculata*) occupy isolated and rather poorly supported positions, mostly close to clades 4 and/or 5.

Our data confirm the idea that many of recently described species have been artificially pushed into the existing taxonomic subdivisions of *Thismia* of Jonker by various authors, including Kumar *et al.* (2017). In fact, some recent discoveries represent completely novel lineages of the genus that most likely merit attribution to separate (undescribed) infrageneric taxa. This is particularly the case for representatives of clade 4 (and to a lesser extent clade 3): of the species found in clade 4, *T. mirabilis* was described in 1965, whereas all the other species were described in the 21st century. This clade was thus completely unknown at the time of Jonker's work (1938, 1948), which is still the widely accepted classification scheme for *Thismia*. In clade 3, only some of the species groups were known to Jonker; in our study, they are represented by a single species, *T. clavigera*, whereas several other species [*T. clandestina* F.Muell., *T. crocea* (Becc.) J.J.Sm. and *T. episcopalis* F.Muell.] are evidently close to some species of clade 3 (i.e. to *T. laevis*, *T. acuminata* and *T. brunneomitra*; Hroneš *et al.*, 2015; Sochor *et al.*, 2018b) on the basis of morphology. As *T. clandestina* is the type species of section *Sarcosiphon*, our data suggest that the representatives of clade 4 were incorrectly attributed

filiformis: S. Chantanaorrapint; *T. mucronata*: M.S. Nuraliev; *T. brunneomitra*: M. Hroneš; *T. rodwayi*: V.S.F.T. Merckx; *T. gongshanensis*: H.-Q. Li.

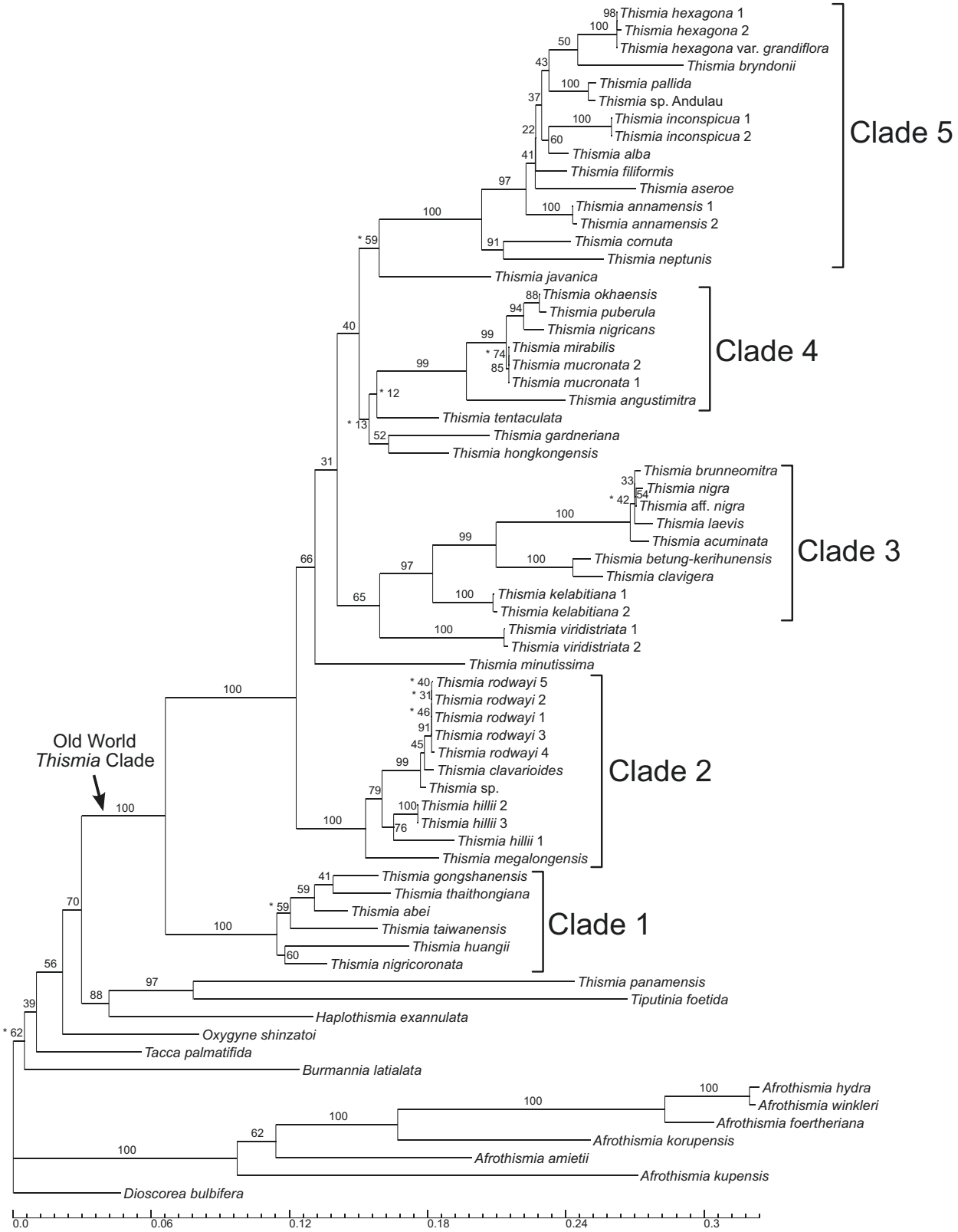

Figure 3. ML tree obtained from the analysis of the combined ITS+18S+*atp1* dataset. Numbers near branches are bootstrap percentage in the maximum likelihood analysis (BP_{ML}); asterisks in front of these numbers indicate the clades that are not supported by Bayesian analysis (Fig. 2).

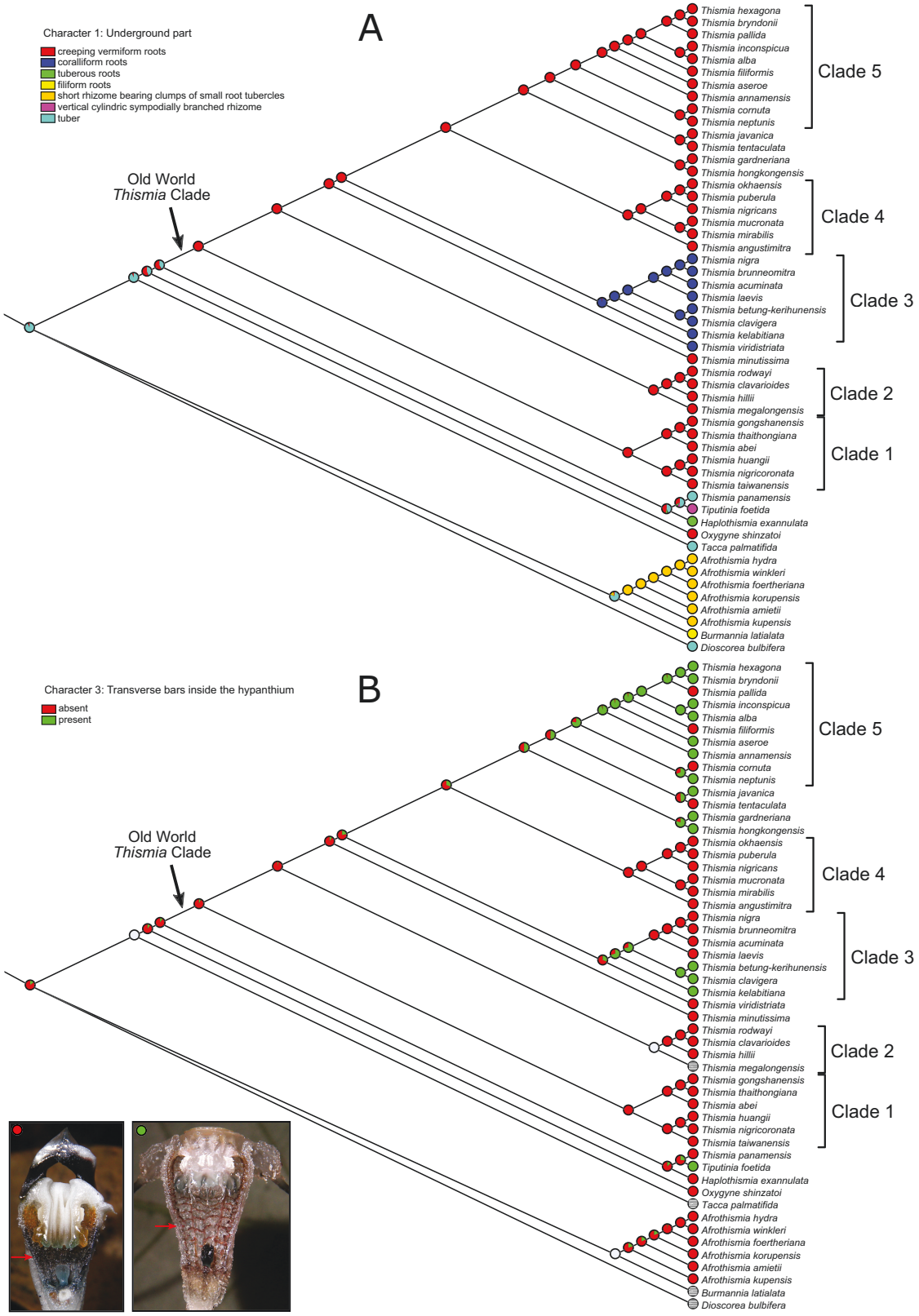

Figure 4. Maximum likelihood ancestral state reconstruction in MESQUITE. A, Character 1: Underground part. B, Character 3: Transverse bars inside the hypanthium. Images: *Thismia mucronata* (left) and *T. annamensis* (right). Character state

to this section, because *T. clandestina* is probably a member of clade 3.

Geographical distribution of species

The five clades of Old World *Thismia* revealed in our study have distribution ranges that are consistent with biogeographic regions; in other words, the distribution of their species differs considerably from the even distribution, and the ranges occupied by the clades are much smaller than the range of the whole genus. This suggests the presence of a phylogenetic signal in the species distribution ranges. Conversely, the ranges of the clades overlap considerably. Some biogeographic regions are inhabited by representatives of a single clade, such as the islands of East Asia (i.e. Japan and Taiwan; clade 1) and south-eastern Australia and New Zealand (clade 2). In Borneo, the centre of the known *Thismia* species diversity, only two clades are found (clades 3 and 5). In contrast, species of four clades occur in mainland South-East Asia (clades 1, 4, 5 and *T. clavigera* of clade 3), although this region is generally poor for *Thismia* spp. apart from the Malay Peninsula (Chantanaorrapint & Sridith, 2007, 2015; Chantanaorrapint & Chantanaorrapint, 2009; Chantanaorrapint, Tetsana & Sridith, 2015; Chantanaorrapint *et al.*, 2016; Chantanaorrapint, 2018; Siti-Munirah, 2018; Siti-Munirah & Dome, 2019), which is known to be floristically close to Borneo. The geographical distribution of the five clades will probably expand as more species are included in future analyses; nevertheless, the geographical data do not contradict the groups revealed from molecular phylogenetic reconstructions and represent a significant and useful addition to characterization of the clades. We argue that a biogeographic reconstruction of Old World *Thismia* in the light of the phylogenetic data would significantly improve our knowledge of evolution of this group. Such an analysis will require broader species sampling, including the most recently described species, and databasing of all known records of the species under study.

Evolution of morphological characters

Our results confirm extensive morphological homoplasy in the Old World *Thismia* clade (Merckx & Smets, 2014), a conclusion closely related to the non-monophyly of the traditional infrageneric taxa evaluated on the basis of morphological features. Most of the state changes in this clade consist of accumulation of floral features that make the flower structure more complicated, and these probably act as adaptations for pollination. These are as follows: origin of floral zygomorphy (three times; see also Supporting Information, Supplementary Fig. 11); origin of transverse bars inside the hypanthium (uncertain but multiple times; Fig. 4B); origin of the mitre through postgenital tepal fusion or of a loose dome through tepal overlapping (about six transformations altogether, but there is also a reversal to free inner tepals in a large group containing clade 5; Fig. 5A); and the origin of appendages of outer tepals (most probably four times; Fig. 6B). The loss of structures is much less frequent and occurs for the appendages of the inner tepals (most probably four times; Fig. 6A). In addition, the apparent complete loss of the outer tepals occurred in a subclade of clade 3.

The stamen tube probably originated at the origin of the Old World *Thismia* clade and later disappeared in two species of clade 1 (see also Supporting Information, Supplementary Fig. 14). However, it should be noted that ancestral state reconstruction of this character appears to be highly sensitive to the species sampling in clade 1. For example, if two additional species of this clade with free stamens are included in the analysis, a more plausible hypothesis would be that on the independent origin of the stamen tube in the clade sister to clade 1 and in the corresponding species of clade 1 (without any reversal events). The interstaminal glands appeared after the first divergence event in the Old World clade, i.e. in the clade sister to clade 1 (Fig. 7A). This character seems to be morphologically dependent on the stamens fusing into a tube, as long as the glands are arranged at the sutures of connective fusion. However, similar glands (commonly described as globoid lobes; Woodward *et al.*, 2007; Merckx *et al.*, 2013) are also found in *Tiputinia foetida* P.E.Berry & C.L.Woodw., which is coded here as having free stamen connectives. Conversely, the presence of the glands may indirectly indicate the actual presence of a short basal filament tube in *Tiputinia*, which is consistent with available illustrations, but cannot be proven without morphological examination of this plant. In our reconstruction, the evolution of the interstaminal glands is homologous (non-homoplastic) in the Old World *Thismia* clade, but interstaminal glands are also found in *Tiputinia*. It should be noted that the glands are sometimes hardly discernible and are often overlooked when a careful examination is not conducted; in the current study, we had to re-evaluate this character for several species against their original descriptions. The wing-like appendage of a connective appeared once in a large clade in the Old World clade, simultaneously with interstaminal glands (Fig. 7B). This character represents a rare case of fully non-homoplastic morphological

probabilities are mapped on the resulting Bayesian trees. Lined circles, unknown or non-applicable. Light grey circles in nodes, computation of proportional likelihoods impossible.

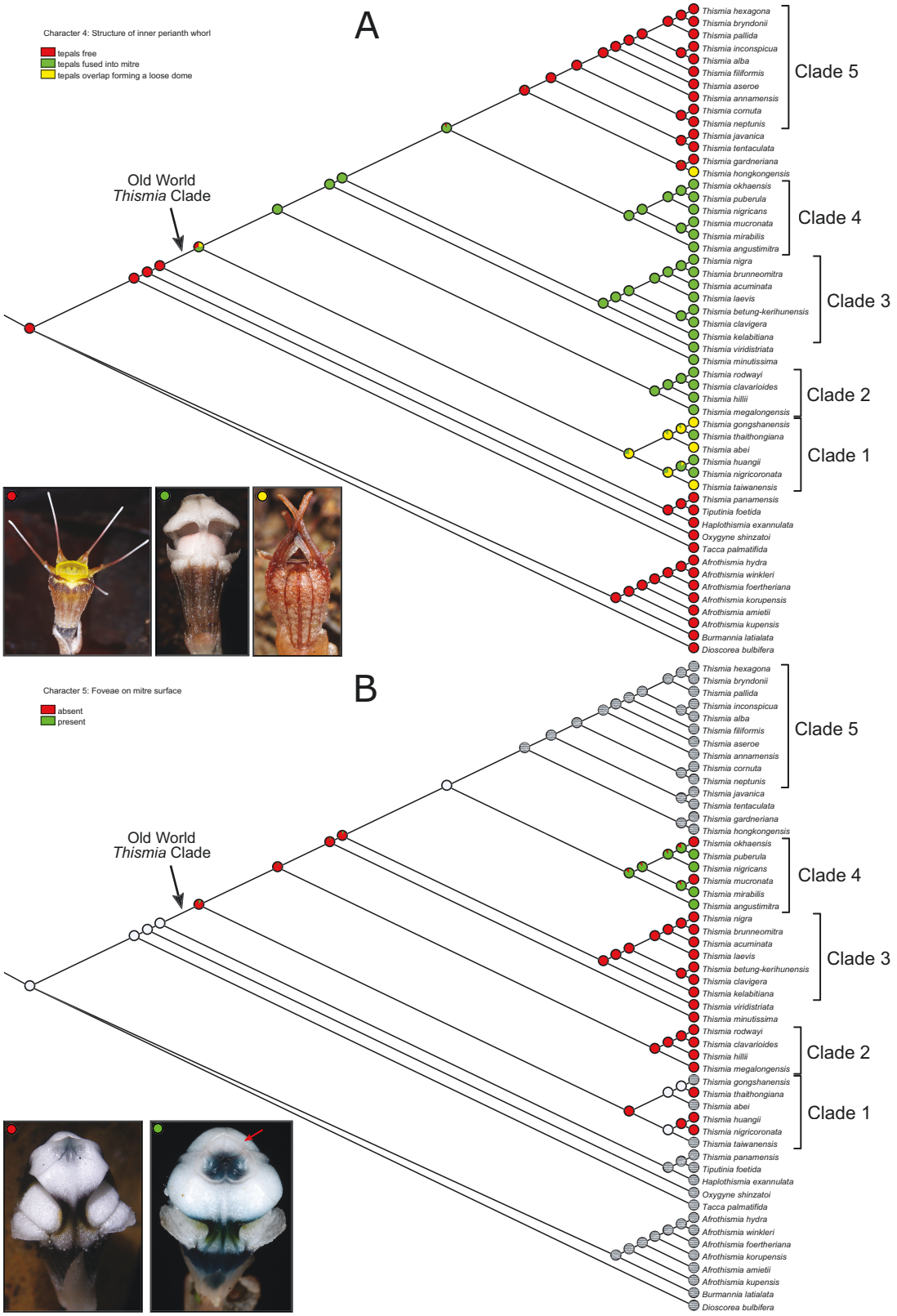

Figure 5. Maximum likelihood ancestral state reconstruction in MESQUITE. A, Character 4: Structure of inner perianth whorl. Images (from left to right): *Thismia hexagona*, *T. puberula*, *T. hongkongensis*. B, Character 5: Foveae on mitre surface.

evolution in Thismiaceae, at least in the samples of species used here. With respect to the characters of the androecium, clade 1 shows considerable morphological similarity with the other studied Dioscoreales, which can be seen as one more piece of evidence for the gradual accumulation of floral complexity in the Old World *Thismia* clade.

The distribution of two floral characters (the presence of appendages of inner tepals and the presence of hypanthium bars, along with several additional ones) is consistent with the recognition of two subclades in clade 3. One of these subclades, consisting of *T. betung-kerihunensis* and *T. clavigera*, is characterized by the presence of both structures and is already treated as *Thismia* section *Geomitra*. The other subclade comprising *T. acuminata*, *T. brunneomitra*, *T. laevis* and *T. nigra* lacks these structures, and it seems to be consistent with *Thismia* section *Sarcosiphon sensu* Jonker (1938), but this disagrees with the expanded limits of this section proposed by Kumar *et al.* (2017). *Thismia betung-kerihunensis* and *T. clavigera* also share some additional features (not studied here), such as the presence of a prominent longitudinal inner rib on the stamen connective.

Our reconstruction of the evolution of the inner perianth whorl allows speculations on the origin of the peculiar structural type treated here as 'tepals overlap forming a loose dome'. From a morphological point of view, the loose dome is closer to free inner tepals, as long as there is no fusion between the tepals. Molecular data suggest that the loose dome has evolved at least twice in the course of the evolution of *Thismia*. One of these cases is *T. hongkongensis*: according to its current placement in our phylogenetic reconstruction, its loose dome originated from free inner tepals, but its phylogenetic position is rather poorly supported. All other species with a loose dome belong to clade 1. It is possible that this feature represents a synapomorphy of clade 1, although the precise reconstruction of its evolution is highly dependent on rather arbitrary decisions regarding character coding. In particular, the flowers with a mitre show considerable morphological heterogeneity, some of them approaching the case of loose dome. In most of the species with a mitre, the aestivation of the inner tepals is valvate, similar to that in species with free inner tepals (M.S. Nuraliev, personal observations). However, in some species, including *T. nigricoronata* (Kumar *et al.*, 2017) and probably all four species of clade 2 (Mueller, 1890a, b; Hunt *et al.*, 2014, V.S.F.T. Merckx, personal observations), the aestivation of the inner tepals is imbricate or contort, i.e. the tepals overlap each other and their margins are clearly discernible within the mitre. At least in some of these species, the tepals can be easily separated (Jonker, 1938). The same pattern of aestivation of the inner perianth whorl is characteristic of species with a loose dome (Akasawa, 1950; Yang, Saunders & Hsu, 2002; Li & Bi, 2013; Mar & Saunders, 2015). The example of *T. nigricoronata* is particularly instructive for illustration of the mitre diversity, as the mitre of this species possesses a central orifice (Kumar *et al.*, 2017), a feature that probably cannot appear in a mitre of valvate tepals and so far is unknown in any other *Thismia* spp. We believe that the structural diversity of the inner perianth whorl in this genus merits further investigations. In subsequent studies, it may appear beneficial to study its evolution by means of the ancestral state reconstruction with consideration of additional characters, including the tepal aestivation.

Notwithstanding the minor uncertainties, our reconstruction at the origin of the Old World clade shows that the loose dome could have originated either from the free inner tepals or from the mitre. In other words, these three conditions seem to be equally close to each other phylogenetically, despite the loose dome resembling free tepals in its structure and mitre in its appearance. The possibility of various transitions between these conditions should be taken into account when judging species relationships (and taxonomic placement) on the basis of morphology.

The uncertain positions of *T. gardneriana*, *T. javanica* and *T. tentaculata* in our molecular phylogenetic reconstructions should be discussed in light of their unusual flower structure. Generally, their flowers are morphologically similar to those of clade 5 (to which they all are closely related according to the Bayesian tree), with the main difference being the absence of appendages on their outer tepals. These species are thus unique within our sampling in having free inner tepals (which always coincides with the presence of appendages of inner tepals) and outer tepals without appendages. This kind of perianth morphology falls under the state 'free perianth lobes strongly different in shape and size' in the coding system of Merckx & Smets (2014); however, under this state, they appear to be mixed with some species possessing inner and outer tepal appendages, such as *T. neptunis* (which belongs to clade 5 in our study). On the basis of the same character, all species possessing free inner tepals and lacking appendages of outer tepals plus *T. hongkongensis* and *T. neptunis* were treated under *Thismia* section

Images: *Thismia mucronata* (left) and *T. mirabilis* (right). Character state probabilities are mapped on the resulting Bayesian trees. Lined circles: unknown or non-applicable. Light grey circles in nodes: computation of proportional likelihoods impossible.

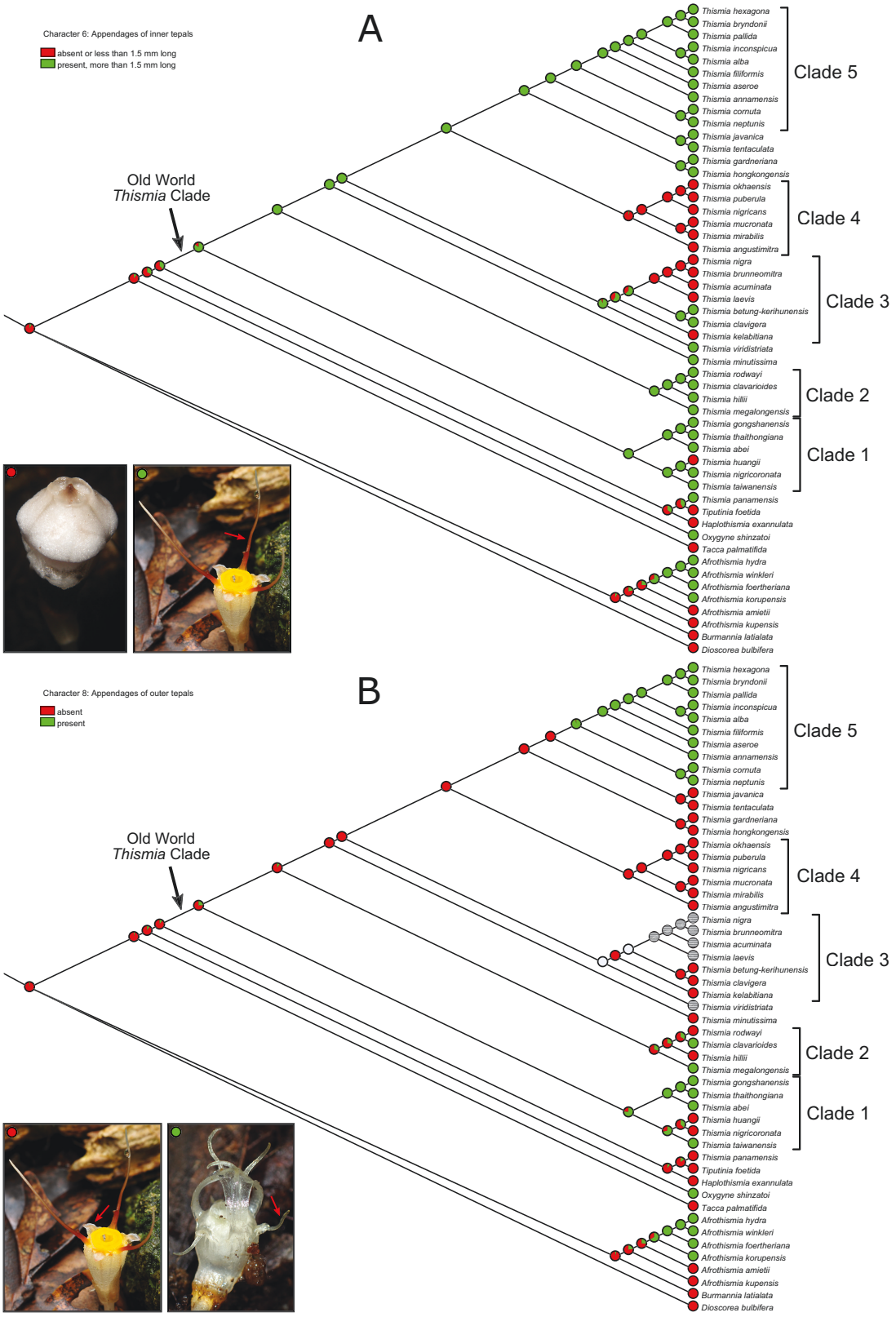

Figure 6. Maximum likelihood ancestral state reconstruction in MESQUITE. A, Character 6: Appendages of inner tepals. Images: *Thismia puberula* (left), *T. tentaculata* (right). B, Character 8: Appendages of outer tepals. Images: *Thismia*

Thismia subsect. *Brunonithismia* (Kumar *et al.*, 2017). As shown in our study, this subsection is polyphyletic and is also significantly heterogeneous with respect to perianth morphology.

Phylogenetic analysis in mycoheterotrophic species and the issue of contamination

Many mycoheterotrophic plants are small slender plants, from which it is difficult to obtain enough material for DNA extraction (especially if the specimen is also intended for morphological description). Additionally, their mycoheterotrophic lifestyle could often lead to contamination of DNA samples with fungal DNA. The contamination by other plants was also reported (Lam *et al.*, 2016). All of these factors sometimes hamper phylogenetic analysis with the first-generation sequencing approach (i.e. based on sequencing of amplified marker regions). New methods of DNA sequencing (high-throughput sequencing approaches; HTS) that have emerged during the last ten years are much less demanding regarding DNA quality than PCR-based sequencing. Additionally, they allow for the identification of marker sequences in complex mixes without their physical separation (e.g. by cloning). Using HTS, we obtained marker sequences from four samples (the type of *T. annamensis*, *T. hexagona*, *T. okhaensis* and *T. tentaculata*) that were unattainable with Sanger sequencing. In the case of *T. hexagona*, the sequences of two plant species were obtained, one of which is *Thismia* itself, and the second, according to the ITS sequence, is *Epirixanthes elongata* Blume. Some authors (see e.g. Sochor *et al.*, 2018b) noted that *Epirixanthes* Blume often co-occurs with *Thismia* spp. *Epirixanthes* is a genus of mycoheterotrophic plants from the distant eudicot family Polygalaceae (Dančák *et al.*, 2017), and it is unlikely that it could be mixed with *Thismia* during collection. We suggest that the source of this contamination is pollen from plants of *E. elongata* growing nearby. Indeed, plant pollen is ubiquitous, and precautions against such contamination are rarely taken during collection. Thus, pollen contamination may be quite frequent when working with plant material collected from natural habitats. Alternatively, contamination due to cross-handling by the collector who sampled both *Thismia* and *Epirixanthes* may occur. The sample of *T. okhaensis* also included DNA of another plant that cannot be reliably identified but presumably belongs to Balanophoraceae (the 18S sequence has 97% similarity with *Corynaea crassa* Hook.f.), as well as human DNA (suggesting that a collector can be a vector for DNA). This case illustrates the utility of HTS for making available sequences from 'hopeless' samples, such as old herbarium (or fixed) samples with highly degraded DNA or those contaminated with fungi and/or other plants; however, it also emphasizes the need of precautions to be taken to avoid the inclusion of contaminating sequences in the analysis.

CONCLUSIONS AND PROSPECTS

Thismia, as currently circumscribed, is polyphyletic and its Neotropical species probably represent a distinct group, separate from the Old World species. Thus, a potential taxonomic solution for the polyphyly of *Thismia* would be separation of the Neotropical species into a segregated genus, whereas *Thismia s.s.* could be limited to the Old World species, probably with the extinct North American *T. americana* (Merckx & Smets, 2014).

Among Old World *Thismia* spp., we infer five monophyletic groups (clades) that each deserve infrageneric taxonomic status. These groups inhabit well-delineated geographical and floristic regions, specifically mainland South-East Asia (clades 1, 4, 5 and *T. clavigera* of clade 3), the islands of East Asia (clade 1), Borneo (clades 3, 5) and south-eastern Australia and New Zealand (clade 2). The evolution of morphological characters was substantially homoplastic in Old World *Thismia*, but our study provides each of the five groups with a unique morphological description. We propose the following characters as most informative in distinguishing the groups, and sufficient to identify them when used in combination: the structure of the underground organs; the structure of the inner perianth whorl; the presence of appendages of the inner tepals; the presence of stamen appendages and the presence of hypanthium bars. In addition, the state distribution of the presence of appendages of the inner tepals and the presence of hypanthium bars (along with several additional characters not addressed here) corroborates the recognition of two subclades in clade 3. Several *Thismia* spp. could not be assigned with certainty to any of the five clades and require further investigation. The sampling of more species and/or the use of higher-resolution data could help to clarify their phylogenetic affinity and their taxonomic placement in the future. In particular, we consider the inclusion of species with unique morphology (such as *T. appendiculata* Schltr., *T. labiata* J.J.Sm. and *T. sahyadrica* Sujanapal, Robi & Dantas) and samples from regions not yet covered (e.g. South America, north-eastern Australia) to be of the highest priority.

Our study, together with earlier papers, clearly indicates that the current taxonomic system of *Thismia*

tentaculata (left) and *T. abei* (right). Character state probabilities are mapped on the resulting Bayesian trees. Lined circles: unknown or non-applicable. Light grey circles in nodes: computation of proportional likelihoods impossible.

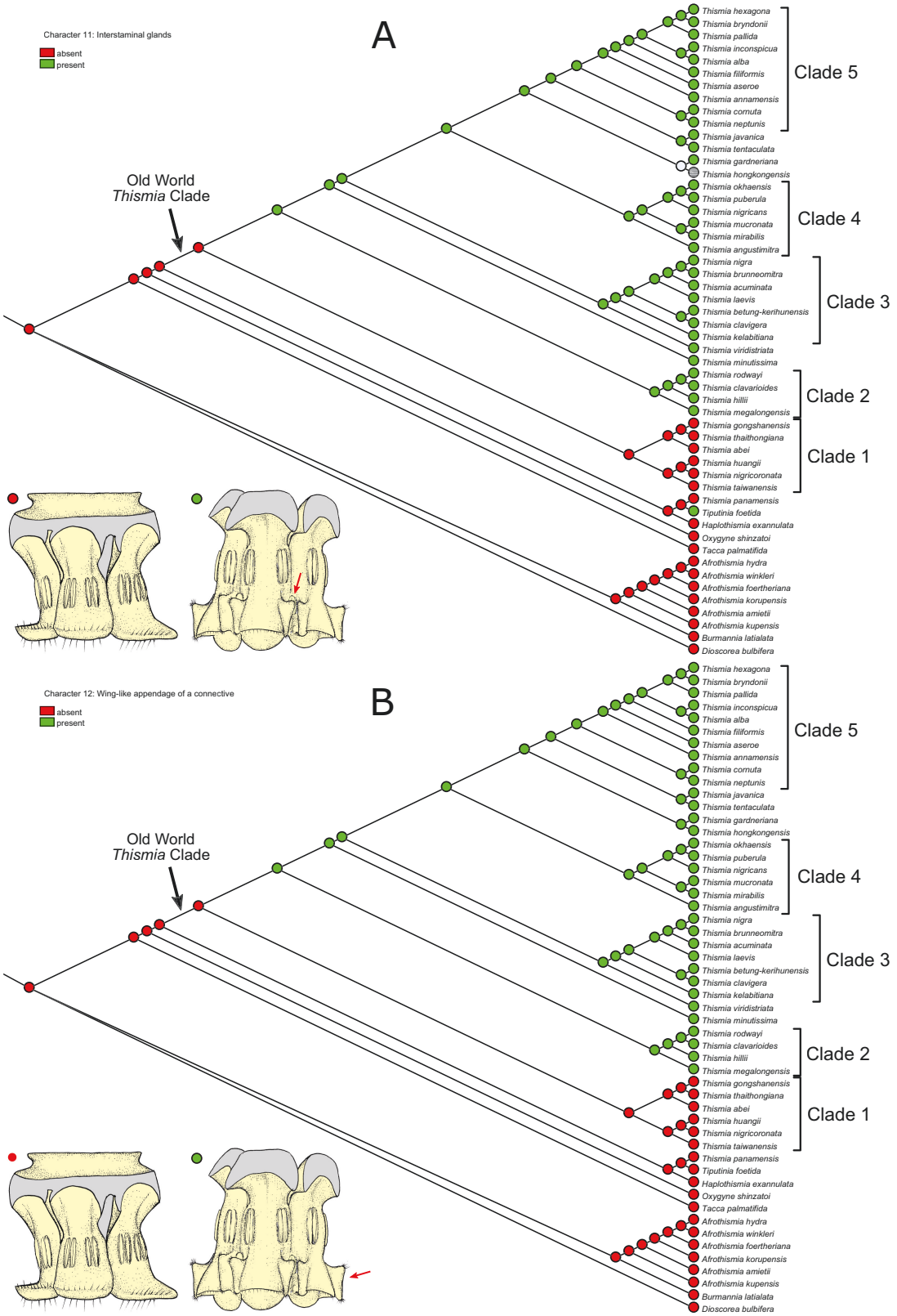

Figure 7. Maximum likelihood ancestral state reconstruction in MESQUITE. A, Character 11: Interstaminal glands. Images: *Thismia thaithongiana* (left), *T. nigricans* (right). B, Character 12: Wing-like appendage of a connective. Images: *Thismia thaithongiana* (left), *T. nigricans* (right). Character state probabilities are mapped on the resulting Bayesian trees.

needs considerable improvement. Notably, the molecular phylogenetic reconstruction appears to be in good agreement with the geographical distribution of species, and at least in some lineages in a better agreement with it than the traditional taxonomic classifications. The phylogenetic signal of geographical patterns was therefore underestimated in the past (e.g. Kumar *et al.*, 2017). Our work provides a basis for such a taxonomic revision and indicates the directions of necessary modifications.

Finally, we propose that the morphological characters studied in this paper, which allow morphological delimitation of monophyletic groups, should receive sufficient attention in the course of further works on the taxonomy of this group. In particular, we suggest that the precise morphological nature of corresponding parts of plants should be evaluated, and uniform terminology should be employed for their description. Such an approach will allow unequivocal coding of the characters for various analyses, as well as more accurate morphological comparison and taxonomic placement of newly described and already existing taxa.

ACKNOWLEDGEMENTS

We thank Gwynne Lim for sharing raw data from genome skimming of *T. tentaculata*; Leonid V. Averyanov for access to the specimen at LE; Sean Graham for reviewing an earlier version of the paper; Sofia Yudina and Richard Saunders for fruitful discussion and two anonymous reviewers for their helpful comments. KS and HT thank the Secretariat of Permission for Foreign Research, the Ministry of Research and Technology, Republic of Indonesia (RISTEK), who kindly gave permission for the field research in West Kalimantan, and the Indonesian Institute of Science (LIPI) and the Betung Kerihun National Park office for kindly allowing this study to take place in Betung Kerihun National Park, West Kalimantan. The study by KS and HT was also performed with the following permission: YS/MBMC/ 2013/50, YS/MBMC/2016/184 and YS/MBMC/2016/200 from the Maliau Basin Management Committee and Access License JKM/ MBS.1000–2/2(152) and JKM/MBS.1000–2/2 JLD.5 (23) from the Sabah Biodiversity Council. The fieldwork of MD, MH and MS was conducted under the permits No. NCCD.907.4.4(JLD.13)-337 and (298)JHS/NCCD/600-7/2/107 issued by Sarawak Forestry Department. We also thank the Brunei Forestry Department and the Biodiversity Research and Innovation Centre, Ministry of Industry and Primary Resources for permission to work at the Ulu Temburong National Park and permit to export specimens, respectively. The work of EAS, MIS, MDL and MSN was supported by the Russian Foundation for Basic Research (project 18-04-00619). MH was supported by Univerzita Palackého v Olomouci (IGA PrF-2020-003). MS was supported by grant No. RO0418 from the Ministry of Agriculture of the Czech Republic. KS and HT were supported by Grant-in-Aid from the Asahi Glass Foundation (2016-11/88). This work was carried out in accordance with government orders for the Lomonosov Moscow State University (project No. AAAA-A16-116021660105-3) and Institute for Information Transmission Problems (project No. 0053-2019-0005).

REFERENCES

Akasawa Y. 1950. A new species of *Glaziocharis* (Burmanniaceae) found in Japan. *Journal of Japanese Botany* **25:** 193–196.

APG III. 2009. An update of the Angiosperm Phylogeny Group classification for the orders and families of flowering plants: APG III. *Botanical Journal of the Linnean Society* **161:** 105–121.

APG IV. 2016. An update of the Angiosperm Phylogeny Group classification for the orders and families of flowering plants: APG IV. *Botanical Journal of the Linnean Society* **181:** 1–20.

Baldwin BG. 1992. Phylogenetic utility of the internal transcribed spacers of nuclear ribosomal DNA in plants: an example from the Compositae. *Molecular Phylogenetics and Evolution* **1:** 3–16.

Borowiec ML. 2016. AMAS: a fast tool for alignment manipulation and computing of summary statistics. *PeerJ* **4:** e1660.

Brazeau MD. 2011. Problematic character coding methods in morphology and their effects. *Biological Journal of the Linnean Society* **104:** 489–498.

Caddick LR, **Rudall PJ**, **Wilkin P**, **Hedderson TAJ**, **Chase MW. 2002.** Phylogenetics of Dioscoreales based on combined analyses of morphological and molecular data. *Botanical Journal of the Linnean Society* **138:** 123–144.

Castresana J. 2000. Selection of conserved blocks from multiple alignments for their use in phylogenetic analysis. *Molecular Biology and Evolution* **17:** 540–552.

Chantanaorrapint S. 2012. *Thismia filiformis*, a new species of Thismiaceae (formerly Burmanniaceae) from Thailand. *Kew Bulletin* **67:** 69–73.

Chantanaorrapint S. 2018. Lectotypification of *Thismia arachnites* (Thismiaceae), a mysterious species newly reported for Thailand. *Kew Bulletin* **73:** 43.

Chantanaorrapint S, **Chantanaorrapint A. 2009.** *Thismia clavigera* (Thismiaceae), a new record for Thailand. *Thai Forest Bulletin (Botany)* **37:** 27–31.

Chantanaorrapint S, **Sridith K. 2007.** *Thismia alba* (Thismiaceae), a new record for Thailand. *Thai Forest Bulletin (Botany)* **35:** 34–37.

Chantanaorrapint S, **Sridith K. 2015.** *Thismia nigricans* Chantanaorr. & Sridith, a new species of Thismiaceae from Southern Thailand. *Phytotaxa* **217:** 293–297.

Chantanaorrapint S, **Suddee S. 2018.** *Thismia thaithongiana* (Dioscoreaceae: Thismieae), a new species of mycoheterotroph from an unusual habitat. *Phytotaxa* **333:** 287–292.

Chantanaorrapint S, **Tetsana N**, **Sridith K. 2015.** Notes on *Thismia clandestina* (Thismiaceae), a little-known mycoheterotrophic species. *Polish Botanical Journal* **60:** 71–74.

Chantanaorrapint S, **Tetsana N**, **Tripetch P**, **Suddee S. 2019.** *Thismia submucronata* (Thismiaceae), a new species from mainland Southeast Asia. *Taiwania* **64:** 240–244.

Chantanaorrapint S, **Wai JS**, **Poopath M**, **Tetsana N. 2016.** *Thismia claviformis* (Thismiaceae), a new species from the Thai-Malay Peninsula. *Phytotaxa* **280:** 292–296.

Cheek M, **Etuge M**, **Williams SA. 2019.** *Afrothismia kupensis* sp. nov. (Thismiaceae), critically endangered, with observations on its pollination and notes on the endemics of Mt Kupe, Cameroon. *Blumea* **64:** 158–164.

Cheek M, **Tsukaya H**, **Rudall PJ**, **Suetsugu K. 2018.** Taxonomic monograph of *Oxygyne* (Thismiaceae), rare achlorophyllous mycoheterotrophs with strongly disjunct distribution. *PeerJ* **6:** e4828.

Dančák M, **Hroneš M**, **Sochor M. 2020.** *Thismia ornata* and *T. coronata* (Thismiaceae), two new species from Sarawak, Borneo. *Willdenowia* **50:** 65–76.

Dančák M, **Hroneš M**, **Sochor M**, **Sochorová Z. 2018.** *Thismia kelabitiana* (Thismiaceae), a new unique fairy lantern from Borneo potentially threatened by commercial logging. *PLoS One* **13:** e0203443.

Dančák M, **Hroneš M**, **Sukri RS**, **Metali F**, **Joffre AA. 2017.** Novitates bruneienses, 9. A synopsis of *Epirixanthes* (Polygalaceae) in Brunei Darussalam and notes on species elsewhere. *Gardens' Bulletin Singapore* **69:** 179–187.

Davis JI, **Stevenson DW**, **Petersen G**, **Seberg O**, **Campbell LM**, **Freudenstein JV**, **Goldman DH**, **Hardy CR**, **Michelangeli FA**, **Simmons MP**, **Specht CD**, **Vergara-Silva F**, **Gandolfo M. 2004.** A phylogeny of the monocots, as inferred from *rbcL* and *atpA* sequence variation, and a comparison of methods for calculating jackknife and bootstrap values. *Systematic Botany* **29:** 467–510.

Doyle JJ, **Doyle JM. 1987.** A rapid DNA isolation procedure for small quantities of fresh leaf tissue. *Phytochemical Bulletin, Botanical Society of America* **19:** 11–15.

Griffith W. 1845. XXVII. On the root-parasites referred by authors to Rhizantheae; and on various plants related to them. *Transactions of the Linnean Society of London* **19:** 303–347.

Hershkovitz M, **Hahn WJ**, **Zimmer EA. 1999.** Ribosomal DNA evolution and plant systematics. In: Hollingsworth P, Bateman R, Gornall R, eds. *Advances in plant molecular systematics*. London: Taylor & Francis, 268–326.

Hroneš M, **Kobrlová L**, **Taraška V**, **Popelka O**, **Hédl R**, **Sukri RS**, **Metali F**, **Dančák M. 2015.** *Thismia brunneomitra*, another new species of *Thismia* (Thismiaceae) from Ulu Temburong, Brunei Darussalam. *Phytotaxa* **234:** 172–178.

Hunt C, **Steenbeeke G**, **Merckx V. 2014.** *Thismia megalongensis* (Thismiaceae), a new species of *Thismia* from New South Wales. *Telopea* **16:** 165–174.

Jonker FP. 1938. A monograph of the Burmanniaceae. *Mededeelingen van het Botanisch Museum en Herbarium van de Rijks Universiteit te Utrecht (Utrecht)* **51:** 1–279.

Jonker FP. 1948. Burmanniaceae. In: van Steenis CGGJ, ed. *Flora Malesiana*. Batavia: Noordhoff-Kolff N.V., 12–26.

Katoh K, **Standley DM. 2013.** MAFFT multiple sequence alignment software version 7: improvements in performance and usability. *Molecular Biology and Evolution* **30:** 772–780.

Kumar P, **Gale SW**, **Li JH**, **Bouamanivong S**, **Fischer GA. 2017.** *Thismia nigricoronata*, a new species of Burmanniaceae (Thismieae, Dioscoreales) from Vang Vieng, Vientiane Province, Laos, and a key to subgeneric classification. *Phytotaxa* **319:** 225–240.

Lam VKY, **Darby H**, **Merckx VSFT**, **Lim G**, **Yukawa T**, **Neubig KM**, **Abbott JR**, **Beatty GE**, **Provan J**, **Soto Gomez M**, **Graham SW. 2018.** Phylogenomic inference in extremis: a case study with mycoheterotroph plastomes. *American Journal of Botany* **105:** 480–494.

Lam VKY, **Merckx VSFT**, **Graham SW. 2016.** A few-gene plastid phylogenetic framework for mycoheterotrophic monocots. *American Journal of Botany* **103:** 692–708.

Lanfear R, **Frandsen PB**, **Wright AM**, **Senfeld T**, **Calcott B. 2017.** PartitionFinder 2: new methods for selecting partitioned models of evolution for molecular and morphological phylogenetic analyses. *Molecular Biology and Evolution* **34:** 772–77.

Li HQ, **Bi YK. 2013.** A new species of *Thismia* (Thismiaceae) from Yunnan, China. *Phytotaxa* **105:** 25–28.

Lim GS, **Barrett CF**, **Pang CC**, **Davis JI. 2016.** Drastic reduction of plastome size in the mycoheterotrophic *Thismia tentaculata* relative to that of its autotrophic relative *Tacca chantrieri*. *American Journal of Botany* **103:** 1129–1137.

Maas PJM, **Maas-van de Kamer H**, **van Benthem J**, **Snelders HCM**, **Rübsamen T. 1986.** Burmanniaceae. *Flora Neotropica* **42:** 1–189.

Maas-Van de Kamer H. 1998. Burmanniaceae. In: Kubitzki K, ed. *Families and genera of vascular plants, Vol. 3: Monocotyledons, Lilianae (except Orchidaceae)*. Berlin, Heidelberg, New York: Springer, 154–164.

Maddison WP, **Maddison DR. 2006.** StochChar: a package of Mesquite modules for stochastic models of character evolution. http://www.mesquiteproject.org.

Maddison WP, **Maddison DR. 2018.** *Mesquite: a modular system for evolutionary analysis*. http://www.mesquiteproject.org.

Mar SS, **Saunders R. 2015.** *Thismia hongkongensis* (Thismiaceae): a new mycoheterotrophic species from Hong Kong, China, with observations on floral visitors and seed dispersal. *PhytoKeys* **46:** 21–33.

Merckx VSFT, **Bakker FT**, **Huysmans S**, **Smets E. 2009.** Bias and conflict in phylogenetic inference of myco-heterotrophic plants: a case study in Thismiaceae. *Cladistics* **25:** 64–77.

Merckx VSFT, **Bidartondo MI. 2008.** Breakdown and delayed cospeciation in the arbuscular mycorrhizal mutualism. *Proceedings of the Royal Society B: Biological Sciences* **275:** 1029–1035.

Merckx VSFT, **Chatrou LW**, **Lemaire B**, **Sainge MN**, **Huysmans S**, **Smets EF. 2008.** Diversification of myco-heterotrophic angiosperms: evidence from Burmanniaceae. *BMC Evolutionary Biology* **8:** 178.

Merckx VSFT, **Freudenstein JV**, **Kissling J**, **Christenhusz MJM**, **Stotler RE**, **Crandall-Stotler B**,

Wickett N, **Rudall PJ**, **Maas-van de Kamer H**, **Maas PJM. 2013.** Taxonomy and classification. In: Merckx V, ed. *Mycoheterotrophy: the biology of plants living on fungi*. New York: Springer New York, 19–101.

Merckx VSFT, **Gomes SIF**, **Wapstra M**, **Hunt C**, **Steenbeeke G**, **Mennes CB**, **Walsh N**, **Smissen R**, **Hsieh TH**, **Smets EF**, **Bidartondo MI. 2017.** The biogeographical history of the interaction between mycoheterotrophic *Thismia* (Thismiaceae) plants and mycorrhizal *Rhizophagus* (Glomeraceae) fungi. *Journal of Biogeography* **44:** 1869–1879.

Merckx VSFT, **Huysmans S**, **Smets E. 2010.** Cretaceous origins of myco-heterotrophic lineages in Dioscoreales. In: Seberg O, Petersen G, Barfod AS, Davis J, eds. *Diversity, phylogeny, and evolution in the monocotyledons*. Århus: Aarhus University Press, 39–53.

Merckx VSFT, **Schols P**, **Maas-van de Kamer H**, **Maas P**, **Huysmans S**, **Smets E. 2006.** Phylogeny and evolution of Burmanniaceae (Dioscoreales) based on nuclear and mitochondrial data. *American Journal of Botany* **93:** 1684–1698.

Merckx VSFT, **Smets EF. 2014.** *Thismia americana*, the 101st anniversary of a botanical mystery. *International Journal of Plant Sciences* **175:** 165–175.

Mueller FJHV. 1890a. Description of new Australian plants with occasional, other annotations. *The Victorian Naturalist* **7:** 114–116.

Mueller FJHV. 1890b. Notes on a new Tasmanian plant of the order Burmanniaceae. *Papers and Proceedings of the Royal Society of Tasmania* **1890:** 232–235.

Nuraliev MS, **Beer AS**, **Kuznetsov AN**, **Kuznetsova SP. 2014.** *Thismia mucronata* (Thismiaceae), a new species from southern Vietnam. *Phytotaxa* **167:** 245–255.

Nuraliev MS, **Beer AS**, **Kuznetsov AN**, **Kuznetsova SP. 2015.** *Thismia puberula* (Thismiaceae), a new species from southern Vietnam. *Phytotaxa* **234:** 133–142.

Oetting WS, **Lee HK**, **Flanders DJ**, **Wiesner GL**, **Sellers TA**, **King RA. 1995.** Linkage analysis with multiplexed short tandem repeat polymorphisms using infrared fluorescence and M13 tailed primers. *Genomics* **30:** 450–458.

Rambaut A, **Drummond AJ**, **Xie D**, **Baele G**, **Suchard MA. 2018.** Posterior summarization in Bayesian phylogenetics using Tracer 1.7. *Systematic Biology* **67:** 901–904.

Ronquist F, **Teslenko M**, **van der Mark P**, **Ayres DL**, **Darling A**, **Höhna S**, **Larget B**, **Liu L**, **Suchard MA**, **Huelsenbeck JP. 2012.** MrBayes 3.2: efficient Bayesian phylogenetic inference and model choice across a large model space. *Systematic Biology* **61:** 539–542.

Rubinoff D, **Holland BS. 2005.** Between two extremes: mitochondrial DNA is neither the panacea nor the nemesis of phylogenetic and taxonomic inference. *Systematic Biology* **54:** 952–961.

Scarcelli N, **Barnaud A**, **Eiserhardt W**, **Treier UA**, **Seveno M**, **d'Anfray A**, **Vigouroux Y**, **Pintaud JC. 2011.** A set of 100 chloroplast DNA primer pairs to study population genetics and phylogeny in Monocotyledons. *PLoS One* **6:** e19954.

Siti-Munirah MY. 2018. *Thismia kelantanensis* (Thismiaceae), a new species from Kelantan, Peninsular Malaysia. *Kew Bulletin* **73:** 42.

Siti-Munirah MY, **Dome N. 2019.** *Thismia domei* and *T. terengganuensis* (Thismiaceae), two new species, and *T. javanica*, a new record from Terengganu, Peninsular Malaysia. *PhytoKeys* **124:** 123–137.

Sochor M, **Egertová Z**, **Hroneš M**, **Dančák M. 2018a.** Rediscovery of *Thismia neptunis* (Thismiaceae) after 151 years. *Phytotaxa* **340:** 71–78.

Sochor M, **Hroneš M**, **Dančák M. 2018b.** New insights into variation, evolution and taxonomy of fairy lanterns (*Thismia*, Thismiaceae) with four new species from Borneo. *Plant Systematics and Evolution* **304:** 699–721.

Sochor M, **Sukri RS**, **Metali F**, **Dančák M. 2017.** *Thismia inconspicua* (Thismiaceae), a new mycoheterotrophic species from Borneo. *Phytotaxa* **295:** 263–270.

Stamatakis A. 2014. RAxML version 8: a tool for phylogenetic analysis and post-analysis of large phylogenies. *Bioinformatics* **30:** 1312–1313.

Stevens PF. 2001. *Angiosperm phylogeny website. Version 14*. Available at: http://www.mobot.org/MOBOT/research/APweb/.

Stöver BC, **Müller KF. 2010.** TreeGraph 2: combining and visualizing evidence from different phylogenetic analyses. *BMC Bioinformatics* **11:** 7.

Straub SCK, **Parks M**, **Weitemier K**, **Fishbein M**, **Cronn RC**, **Liston A. 2012.** Navigating the tip of the genomic iceberg: next-generation sequencing for plant systematics. *American Journal of Botany* **99:** 349–364.

Suetsugu K, **Tsukaya H**, **Nurainas N**, **Okada H. 2018.** *Thismia sumatrana* (Thismiaceae), a new species from West Sumatra, Indonesia, with discussions on the taxonomic identity of *Thismia clavigera*. *PhytoKeys* **113:** 59–67.

Swofford DL, **Waddell PJ**, **Huelsenbeck JP**, **Foster PG**, **Lewis PO**, **Rogers JS. 2001.** Bias in phylogenetic estimation and its relevance to the choice between parsimony and likelihood methods. *Systematic Biology* **50:** 525–539.

Thiele K, **Jordan P. 2002.** *Thismia clavarioides* (Thismiaceae), a new species of fairy lantern from New South Wales. *Telopea* **9:** 765–771.

Tsukaya H, **Okada H. 2012.** A new species of *Thismia* (Thismiaceae) from West Kalimantan, Borneo. *Systematic Botany* **37:** 53–57.

White TJ, **Bruns T**, **Lee S**, **Taylor JW. 1990.** Amplification and direct sequencing of fungal ribosomal RNA genes for phylogenetics. In: Innis MA, Gelfand DH, Sninsky JJ, White TJ, eds. *PCR protocols: a guide to methods and applications*. New York: Academic Press Inc., 315–322.

Woodward CL, **Berry PE**, **de Kamer HM van**, **Swing K. 2007.** *Tiputinia foetida*, a new mycoheterotrophic genus of Thismiaceae from Amazonian Ecuador, and a likely case of deceit pollination. *Taxon* **56:** 157–162.

Yang SZ, **Saunders RMK**, **Hsu CJ. 2002.** *Thismia taiwanensis* sp. nov. (Burmanniaceae tribe Thismieae): first record of the tribe in China. *Systematic Botany* **27:** 485–488.

Yokoyama J, **Koizumi Y**, **Yokota M**, **Tsukaya H. 2008.** Phylogenetic position of *Oxygyne shinzatoi* (Burmanniaceae) inferred from 18S rDNA sequences. *Journal of Plant Research* **121:** 27–32.

Zhang L, **Li HT**, **Gao LM**, **Yang JB**, **Li DZ**, **Cannon CH**, **Chen J**, **Li QJ. 2011.** Phylogeny and evolution of bracts and bracteoles in *Tacca* (Dioscoreaceae). *Journal of Integrative Plant Biology* **53:** 901–911.

APPENDIX 1. Species and gene regions sequenced for this study, voucher information, geographic origin, geographical range and GenBank accession numbers

Species	Geographical origin of the sequenced material	Voucher	Source or label data	ITS GenBank number	18S GenBank number	*atp1* GenBank number
Thismia abei (Akasawa) Hatus.	Japan	*K. Suetsugu s.n.*	Kohzu Island, Kohzu village, Tokyo pref., 34°13'02"N 136°14'03"E, 18.08.2015	MK356135	MK356115	MN072714
Thismia acuminata Hroneš, Dančák & Sochor	Malaysia, Borneo	*M. Sochor, M. Hroneš, M. Dančák, Z. Egertová, D. Atu BOR6/17* (SAR, holotype)	ITS, 18S, *atp1*: Sochor *et al.*, 2018b	MG008338[a]	MG008350[a]	MG008365[a]
Thismia alba Holttum ex Jonker	Thailand	*S. Chantanaorrapint 2801* (PSU)	Songkhla prov., Ton Nga Chang waterfall, *c.* 500 m, 6°99'N 100°22'E, 04.10.2013	MK356123	MK356101	MN072704
Thismia angustimitra Chantanaorr.	Thailand	*S. Chantanaorrapint, C. Promma 3904* (BKF, PSU)	Bueng Kan prov., Bungkhla, Phu Wua Wildlife Sanctuary, Nature trail from headquarter, 190–300 m, 18°14'19.40" N 103°57'47.02"E, 16.08.2014	MK356124	-	-
Thismia annamensis K.Larsen & Aver. 1	Vietnam	*M.S. Nuraliev 999* (MW)	Dak Lak prov., Lak distr., Bong Krang munic., Chu Yang Sin national park, 12 km S of Krong Kmar village, forest, small river bank, *c.* 1100 m, 12°23'41"N 108°20'55"E, 28.05.2014	MK356125	MK356102	MN072705
Thismia annamensis K.Larsen & Aver. 2	Vietnam	*L. Averyanov, T.V. Thao, N.T. Vinh HLF 5510* (LE, holotype)	Dak Nong prov., Dak Glong distr., Dak Plao munic., Ta Dung Nature Reserve, *c.* 700–750 m, 11°51'47"N 107°56'59"E, 04.11.2005	MK356141	MK356119	MN072719
Thismia aseroe Becc.[b]	Malaysia, Borneo	*L. Caddick 349* (SAR)	ITS: Merckx *et al.*, 2017; 18S: Caddick *et al.*, 2002; *atp1*: Merckx & Bidartondo, 2008	KY554877[a]	AF309404[a]	EU421048[a]
Thismia betung-kerihunensis Tsukaya & H.Okada	Indonesia, Borneo	*H. Okada, H. Nagamasu, H. Tsukaya HT1012* (BO, holotype)	West Kalimantan, Betung Kerihun National Park, near Sungai (River) Tobong Kopang, *c.* 228 m, on slope under tropical rain forest (lower hill forest) mainly composed of Dipterocarpaceae, 00°54'51.1"N 113°40'20.7"E, 27.12.2010	MK356140	-	-
Thismia brunneomitra Hroneš, Kobrlová & Dančák	Brunei	*M. Dančák MD-Bru/17*	ITS, 18S, *atp1*: Sochor *et al.*, 2018b	MG765546[a]	MG765546[a]	MG765544[a]

APPENDIX 1. Continued

Species	Geographical origin of the sequenced material	Voucher	Source or label data	ITS GenBank number	18S GenBank number	*atp1* GenBank number
Thismia bryndonii Tsukaya, Suetsugu & Suleiman	Malaysia, Borneo	*H. Tsukaya, K. Suetsugu, M. Suleiman TSS-14* (BORH, holotype)	Sabah, Maliau Basin Conservation Area, along the Belian Trail, elevation *c*. 260 m, 04°41'50"N 116°54'27"E, 30.09.2016	MK356143	-	-
Thismia clavarioides K.R.Thiele	Australia	*P. Jordan NSW 447624* (NSW, holotype)	ITS: Merckx *et al.*, 2017; 18S, *atp1*: Merckx & Smets, 2014	KX790903[a]	KF692533[a]	KF692539[a]
Thismia clavigera F.Muell.	Malaysia, Borneo	*L. Caddick 354* (K, although absent from there according to Suetsugu *et al.*, 2018)	ITS: Merckx *et al.*, 2017; 18S: Caddick *et al.*, 2002; *atp1*: Merckx & Bidartondo, 2008	KY554878[a]	AF309405[a]	EU421049[a]
Thismia cornuta Hroneš, Sochor & Dančák	Malaysia, Borneo	*M. Sochor, M. Hroneš, M. Dančák, Z. Egertová, J.R. Pasan BOR2 / 17* (SAR, holotype)	ITS, 18S, *atp1*: Sochor *et al.*, 2018b	MG008341[a]	MG008353[a]	MG008367[a]
Thismia filiformis Chantanaorr.	Thailand	*S. Chantanaorrapint, C. Promma 3928* (PSU)	Prachinburi prov., Khao Yai National Park, Pha Tabak waterfall, *c*. 710 m, 14°21'52.01N 101°20'48.51"E, 19.08.2014	MK356126	MK356103	MN072706
Thismia gardneriana Hook.f. ex Thwaites	Thailand	*S. Chantanaorrapint, C. Promma 3903* (PSU)	Phangnga prov., Khao Lak National Park, Hin Lad waterfall, *c*. 200 m, 08°35'12.59"N, 098°27'05.22"E, 04.08.2014	MK356127	MK356104	MN072712
Thismia gongshanensis Hong Qing Li & Y.K.Bi	China, Yunnan	*Li 2008128* (HSNU, holotype)	Maku Village, Dulongjiang town, Gongshan county, *c*. 2275 m, 27°41'54.6" N, 98°18'15.62" E, 27.06.2008	MK356144	MK356121	MN072721
Thismia hexagona Dančák, Hroneš, Kobrlová & Sochor 1	Brunei	*M. Hroneš s.n.* (photograph: OL)	Temburong Distr., Kuala Belalong, eastern ridge of Sungai Belalong, near its confluence with Sungai Temburong, ecological plot 1, 04°32.952'N 115°09.792'E, 26.01.2015	MK356138	MK356117	MN072718

APPENDIX 1. Continued

Species	Geographical origin of the sequenced material	Voucher	Source or label data	ITS GenBank number	18S GenBank number	*atp1* GenBank number
Thismia hexagona Dančák, Hroneš, Kobrlová & Sochor 2	Brunei	*M. Sochor s.n.*	ITS: Sochor *et al.*, 2018b; 18S, *atp1*: Sochor *et al.*, 2017	MG008342[a]	KU948543[a]	KU948541[a]
Thismia hexagona var. *grandiflora* Tsukaya, Suleiman & H.Okada	Malaysia, Borneo	*H. Tsukaya, M. Suleiman, H. Okada KKT-1* (BORH, holotype)	Maliau Basin Conservation Area, Sabah, 235 m, from Studies Center to Seraya Camp, Maliau Basin Conservation Area, 04°44'29"N 116°57'55"E, 15.08.2013	MK356146	-	-
Thismia hillii (Cheeseman) N.Pfeiff. 1	New Zealand	*P. Garnock-Jones 2218* (WELTU)	18S: Caddick *et al.*, 2002; *atp1*: Davis *et al.*, 2004	-	AF309403[a]	AY299849[a]
Thismia hillii (Cheeseman) N.Pfeiff. 2	New Zealand	*V. Merckx et al. NZ3_TH2*	ITS, 18S, *atp1*: Merckx *et al.*, 2017	KX790907[a]	KY554862[a]	KY554872[a]
Thismia hillii (Cheeseman) N.Pfeiff. 3	Australia	*V. Merckx et al. NSW1_TH5*	ITS, 18S, *atp1*: Merckx *et al.*, 2017	KX790917[a]	KY554861[a]	KY554871[a]
Thismia hongkongensis Mar & R.M.K. Saunders	China, Hong Kong	*S.S. Mar 3* (HK, paratype)	Tai Po Kau Nature Reserve, New Territories, 22°25'N 114°11'E, 16.11.2015	MK356128	MK356105	MN072713
Thismia huangii P.Y.Jiang & T. H. Hsieh	China, Taiwan	*T.H. Hsieh, P.Y. Chiang 3031* (type)	ITS: Merckx *et al.*, 2017; 18S, *atp1*: Merckx & Smets, 2014	KY554879[a]	KF692534[a]	KF692543[a]
Thismia inconspicua Sochor & Dančák 1	Brunei	*M. Sochor MS1/16* (BRUN, holotype)	Temburong Distr., Kuala Belalong, ridge between Temburong and Belalong river valleys *c.* 1.4 km SE of their confluence, ecological plot 2, 04°32'33"N 115°09'59"E, 30.01.2016	MK356133	MK356110	MN072711
Thismia inconspicua Sochor & Dančák 2	Brunei	*M. Sochor MS1/16* (BRUN, holotype)	ITS, 18S, *atp1*: Sochor *et al.*, 2017	KU948545[a]	KU948544[a]	KU948542[a]
Thismia javanica J.J.Smith	Myanmar	*S. Ruchisansakun 770a_4715* (photograph: L)	2015	MK356136	MK356118	MN072715

APPENDIX 1. Continued

Species	Geographical origin of the sequenced material	Voucher	Source or label data	ITS GenBank number	18S GenBank number	*atp1* GenBank number
Thismia kelabitiana Dančák, Hroneš & Sochor 1	Malaysia, Borneo	*M. Sochor, M. Hroneš, M. Dančák, Z. Egertová, J.R. Pasan BOR1 / 17* (SAR, holotype)	ITS, 18S, *atp1*: Sochor *et al.*, 2018b	MG008343[a]	MG008355[a]	MG008364[a]
Thismia kelabitiana Dančák, Hroneš & Sochor 2	Malaysia, Borneo	*T. Těšitelová s.n.* (photograph: L)	Kelabit Highlands, 03°42'N 115°31'E	MK356137	MK356116	MN072716
Thismia laevis Sochor, Dančák & Hroneš	Malaysia, Borneo	*M. Sochor, M. Hroneš, M. Dančák, Z. Egertová, D. Atu BOR9 / 17* (SAR, holotype)	ITS, 18S, *atp1*: Sochor *et al.*, 2018b	MG008344[a]	MG008356[a]	MG008366[a]
Thismia megalongensis C.A.Hunt, G.Steenbeeke & V.Merckx	Australia	*C. Hunt, G. Steenbeeke s.n.* (NSW, holotype)	ITS: Merckx *et al.*, 2017; 18S, *atp1*: Hunt *et al.*, 2014	KX790923[a]	KJ885661[a]	KJ885662[a]
Thismia minutissima Dančák, Hroneš & Sochor	Malaysia, Borneo	*M. Sochor, M. Hroneš, M. Dančák, Z. Egertová, J.R. Pasan BOR4 / 17* (SAR, holotype)	Sarawak, Kelabit Highlands, Pa'Umor village, Anak Adi Ridge, 4.4 km SSE of village, *c.* 1195 m, 03°42'01"N 115°31'28"E, 13.01.2017	-	MK356113	MN072717
Thismia mirabilis K.Larsen	Thailand	*S. Chantanaorrapint, C. Promma 3927* (PSU)	Prachinburi prov., Khao Yai National Park, Pha Tabak waterfall, *c.* 710 m, 14°21'52.01"N, 101°20'48.51"E, 19.08.2014	MK356129	-	-
Thismia mucronata Nuraliev 1	Vietnam	*M.S. Nuraliev 813* (MW, holotype)	Lam Dong prov., Bao Lam distr., Loc Bac munic., 22.2 km NNW of Bao Loc town, forest, not far from river, *c.* 1000 m, 11°44'18" N 107°43'22" E, 13.04.2013	MK356130	MK356106	MN072707
Thismia mucronata Nuraliev 2	Vietnam	*M.S. Nuraliev 1009* (MW)	Dak Lak prov., Lak distr., Bong Krang munic., Chu Yang Sin National Park, 10 km S of Krong Kmar village, forest, not far from river, 970 m, 12°25' 5"N 108°21'58"E, 21.05.2014	MK356131	MK356107	MN072708

APPENDIX 1. Continued

Species	Geographical origin of the sequenced material	Voucher	Source or label data	ITS GenBank number	18S GenBank number	*atp1* GenBank number
Thismia neptunis Becc.	Malaysia, Borneo	*M. Sochor, Z. Egertová BOR51/17* (OL)	ITS, 18S, *atp1*: Sochor *et al.*, 2018b	MG008345[a]	MG008357[a]	MG008368[a]
Thismia nigra Dančák, Hroneš & Sochor	Malaysia, Borneo	*M. Sochor, Z. Egertová, D. Atu BOR15/17* (SAR, paratype)	Sarawak, Kelabit Highlands, Pa'Lungan village, Arur Dutu, 5.7 km N of village, *c.* 1210 m, 03°51'43"N 115°31'24"E, 19.01.2017; *atp1*: Sochor *et al.*, 2018b	MK356139	MK356112	MG008362[a]
Thismia aff. *nigra*	Malaysia, Borneo	*M. Sochor et al. BOR26/17* (SAR)	ITS, 18S, *atp1*: Sochor *et al.*, 2018b	MG008339[a]	MG008351[a]	MG008361[a]
Thismia nigricans Chantanaorr. & Sridith	Thailand	*S. Chantanaorrapint & C. Promma 3897* (PSU, holotype)	Phangnga prov., Kura Buri, Bang Wan, Sri Phangnga National Park, *c.* 56 m, 08°59'34.06"N 98°27'5.22"E, 03.08.2014	MK356132	MK356108	MN072709
Thismia nigricoronata Kumar & S.W.Gale	Laos	*Gale, Kumar, Santainsy, Phunthavong HNL-KFBG 0099* (HNL, holotype)	18S, *atp1*: Kumar *et al.*, 2017	-	MF589340[a]	MF589341[a]
Thismia okhaensis Luu, Tich, G.Tran & Đinh	Vietnam	*N.T. Tich, T. Gioi, D.Q. Diep, L.H. Truong, N.T. Trung KH 638B* (SGN, holotype)	Khanh Hoa prov., Khanh Son distr., Khanh Son Protection Forest, O Kha Valley, 12°02'57"N 108°59'10"E, 800 m, 12.07.2013	MK356147	-	MN072724
Thismia pallida Hroneš, Dančák & Rejžek	Malaysia, Borneo	*M. Hroneš, M. Dančák BOR62/17*	ITS, 18S, *atp1*: Sochor *et al.*, 2018b	MG008347[a]	MG008359[a]	MG008369[a]
Thismia panamensis (Standl.) Jonker	Panama	*Aizprua 2946* (LV)	ITS, *atp1*: Merckx & Bidartondo, 2008; 18S: Merckx *et al.*, 2006	EU421058[a]	DQ786081[a]	EU421050[a]
Thismia puberula Nuraliev	Vietnam	*M.S. Nuraliev 1000* (MW, holotype)	Dak Lak prov., Lak distr., Bong Krang munic., Chu Yang Sin national park, 12 km S of Krong Kmar village, forest, on islet of small river, *c.* 1100 m, 12°23'41"N 108°20'55"E, 28.05.2014	-	MK356109	MN072710
Thismia rodwayi F.Muell. 1	Australia, Tasmania	*V. Merckx, M. Wapstra TAS3-1* (L)	18S, *atp1*: Merckx & Smets, 2014	-	KF692536[a]	KF692540[a]
Thismia rodwayi F.Muell. 2	Australia, Victoria	*N. Walsh s.n.* (L)	18S, *atp1*: Merckx & Smets, 2014	-	KF692538[a]	KF692541[a]
Thismia rodwayi F.Muell. 3	Australia, Tasmania	*V. Merckx, M. Wapstra TAS10-1* (L)	18S, *atp1*: Merckx & Smets, 2014	-	KF692537[a]	KF692542[a]

APPENDIX 1. Continued

Species	Geographical origin of the sequenced material	Voucher	Source or label data	ITS GenBank number	18S GenBank number	*atp1* GenBank number
Thismia rodwayi F.Muell. 4	Australia, Tasmania	*V. Merckx et al. TAS9_TR5*	ITS, 18S, *atp1*: Merckx *et al.*, 2017	KX790860[a]	KY554864[a]	KY554874[a]
Thismia rodwayi F.Muell. 5	Australia, Victoria	*V. Merckx et al. VIC1_TR1*	ITS, 18S, *atp1*: Merckx *et al.*, 2017	KX790859[a]	KY554865[a]	KY554875[a]
Thismia sp.	Australia, NSW	*V. Merckx NSW4_TR1*	ITS, 18S, *atp1*: Merckx *et al.*, 2017	-	KY554863[a]	KY554873[a]
Thismia sp. Andulau	Brunei	*M.* Dančák 2017/*72* (OL)	Belait district, Andulau Forest Reserve near Sungai Liang, 4°39'17"N 114°31'27"E, 26.11.2017	MK356142	MK356120	MN072720
Thismia taiwanensis Sheng Z.Yang, R.M.K.Saunders & C.J.Hsu	China, Taiwan	*S.-Z. Yang et al. 28981* (PPI, isotype)	ITS: Merckx *et al.*, 2017; 18S: Merckx *et al.*, 2006; *atp1*: Merckx & Bidartondo, 2008	KY554880[a]	DQ786080[a]	EU421051[a]
Thismia tentaculata K.Larsen & Aver.	China, Hong Kong	*G. Lim 31* (NY)	sequences were obtained from HTS data published by Lim *et al.*, 2016	MK356145	MK356122	MN072722
Thismia thaithongiana Chantanaorr. & Suddee	Thailand	*S. Chantanaorrapint 2755* (PSU, paratype)	Tak prov., Umphang, Doi Hua Mot, *c.* 859 m, 15°58'33.7"N 98°50'14.4"E, 13.10.2012	MK356134	MK356111	MN072723
Thismia viridistriata Sochor, Hroneš & Dančák 1	Malaysia, Borneo	*M. Sochor, M. Hroneš, M. Dančák, Z. Egertová, D. Atu BOR11/17* (SAR, holotype)	ITS, 18S, *atp1*: Sochor *et al.*, 2018b	MG008348[a]	MG008360[a]	MG008363[a]
Thismia viridistriata Sochor, Hroneš & Dančák 2	Malaysia, Borneo	*M. Sochor, M. Hroneš, M. Dančák, Z. Egertová, D. Atu BOR12/17* (SAR, paratype)	Sarawak, Kelabit Highlands, Pa'Lungan village, Arur Bedalawid, 3.0 km N of village, *c.* 1164 m, 03°50'15"N 115°31'16"E, 16.01.2017; ITS: Sochor *et al.*, 2018b	MG008349[a]	MK356114	-
Outgroups						
Afrothismia amietii Cheek	Cameroon	*S. Moses 2632* (YA)	*atp1*: Merckx *et al.*, 2017			KY554866[a]
Afrothismia foertheriana T.Franke, Sainge & Agerer	Cameroon	*V. Merckx et al. 126* (BR, former LV)	ITS, 18S, *atp1*: Merckx & Bidartondo, 2008	EU421055[a]	EU420988[a]	EU421002[a]
Afrothismia hydra Sainge & T.Franke	Cameroon	*V. Merckx et al. 115* (BR, former LV)	ITS, 18S, *atp1*: Merckx & Bidartondo, 2008	EU421054[a]	EU420990[a]	EU421004[a]

APPENDIX 1. Continued

Species	Geographical origin of the sequenced material	Voucher	Source or label data	ITS GenBank number	18S GenBank number	*atp1* GenBank number
Afrothismia korupensis Sainge & T.Franke	Cameroon	*V. Merckx et al. 114* (BR, former LV)	ITS, 18S, *atp1*: Merckx & Bidartondo, 2008	EU421053[a]	EU420991[a]	EU421005[a]
Afrothismia kupensis Cheek & S.A.Williams	Cameroon	*V. Merckx et al. 110* (BR, former LV)	ITS, 18S, *atp1*: Merckx & Bidartondo, 2008 (listed as *A. gesnerioides* H.Maas; see Cheek *et al.*, 2019)	EU421057[a]	EU420989[a]	EU421003[a]
Afrothismia winkleri Schltr.	Cameroon	*V. Merckx et al. 106* (BR, former LV)	ITS, 18S, *atp1*: Merckx & Bidartondo, 2008	EU421056[a]	EU420992[a]	EU421006[a]
Burmannia latialata Pobég.	Gabon	*C. Jongkind 5923* (WAG)	ITS, 18S, *atp1*: Merckx *et al.*, 2008	EU816746[a]	DQ786062[a]	EU421017[a]
Dioscorea bulbifera L.	India	ITS: *Sheikh s.n.*; 18S: *Sheikh s.n.* and *Hahn 6968* (WIS); *atp1*: *RBGE 19821960* and *AU3502*	ITS: Sheikh (submitted); 18S: Sheikh *et al.* (submitted) and Hershkovitz *et al.*, 1999; *atp1*: Merckx *et al.*, 2009 and Scarcelli *et al.*, 2011	KX774430[a]	KC921382[a] and AF069203[a]	FJ215775[a] and JF705273[a]
Haplothismia exannulata Airy Shaw	India	*N. Sasidharan, P. Sujanapal 30476* (KFRI)	18S, *atp1*: Merckx *et al.*, 2006	-	DQ786082[a]	EU421037[a]
Oxygyne shinzatoi (Hatus.) C.Abe & Akasawa	Japan	*H. Tsukaya 061008* (TI), *M. Yokota s.n.* (RYU)	18S: Yokoyama *et al.*, 2008	-	AB437090[a]	-
Tacca palmatifida Baker	Bogor BG, cult. (ZL-003); Indonesia (1377)	ITS: *L. Zhang ZL-003* (HITBC); 18S: *M. Chase 1377* (K); *atp1*: *M. Chase 1377* (K) and *L. Zhang ZL-003* (HITBC)	ITS: Zhang *et al.*, 2011; 18S: Merckx *et al.*, 2006; *atp1*: Merckx *et al.*, 2009 and Zhang *et al.*, 2011	JN850572[a]	DQ786084[a]	FJ215774[a] and JN850561[a]
Tiputinia foetida P.E.Berry & C.L.Woodw.	Ecuador	*Alvaro Javier Perez Castaneda s.n.* (LV)	18S, *atp1*: Merckx *et al.*, 2009	-	FJ215764[a]	FJ215770[a]

Herbarium acronyms follow the Index Herbariorum at http://sweetgum.nybg.org/science/ih/.
[a] Sequences taken from GenBank.
[b] This specimen is identified as *Thismia ornata* Dančák, Hroneš & Sochor in a recent publication (Dančák, Hroneš & Sochor, 2020).

APPENDIX 2. Data matrix used in ancestral state reconstruction of *Thismia* and related taxa. Characters and states shown in Appendix 3. ? is unknown; - is not applicable (following Brazeau, 2011).

Taxon/character	1	2	3	4	5	6	7	8	9	10	11	12
Thismia abei	0	1	0	2	-	1	-	1	1	0	0	0
Thismia acuminata	1	0	0	1	0	0	-	-	1	1	1	1
Thismia alba	0	0	1	0	-	1	-	1	1	1	1	1
Thismia angustimitra	0	0	0	1	1	0	-	0	1	1	1	1
Thismia annamensis	0	0	1	0	-	1	-	1	1	1	1	1
Thismia aseroe	0	0	1	0	-	1	-	1	1	1	1	1
Thismia betung-kerihunensis	1	0	1	1	0	1	0	0	1	1	1	1
Thismia brunneomitra	1	0	0	1	0	0	-	-	1	1	1	1
Thismia bryndonii	0	0	1	0	-	1	-	1	1	1	1	1
Thismia clavarioides	0	0	0	1	0	1	-	1	1	1	1	1
Thismia clavigera	1	0	1	1	0	1	0	0	1	1	1	1
Thismia cornuta	0	1	0	0	-	1	-	1	1	1	1	1
Thismia filiformis	0	0	0	0	-	1	-	1	1	1	1	1
Thismia gardneriana	0	0	1	0	-	1	-	0	1	1	1	1
Thismia gongshanensis	0	0	0	2	-	1	-	1	1	0	0	0
Thismia hexagona	0	0	1	0	-	1	-	1	1	1	1	1
Thismia hillii	0	0	0	1	0	1	-	0	1	1	1	1
Thismia hongkongensis	0	0	1	2	-	1	-	0	1	1	?	1
Thismia huangii	0	0	0	1	0	0	-	0	1	1	0	0
Thismia inconspicua	0	1	1	0	-	1	-	1	1	1	1	1
Thismia javanica	0	0	1	0	-	1	-	0	1	1	1	1
Thismia kelabitiana	1	0	1	1	0	0	-	0	1	1	1	1
Thismia laevis	1	0	0	1	0	0	-	-	1	1	1	1
Thismia megalongensis	0	0	?	1	0	1	-	1	1	1	1	1
Thismia minutissima	0	0	0	1	0	1	-	0	1	1	1	1
Thismia mirabilis	0	0	0	1	1	0	-	0	1	1	1	1
Thismia mucronata	0	0	0	1	0	0	-	0	1	1	1	1
Thismia neptunis	0	0	1	0	-	1	-	1	1	1	1	1
Thismia nigra	1	0	0	1	0	0	-	-	1	1	1	1
Thismia nigricans	0	0	0	1	1	0	-	0	1	1	1	1
Thismia nigricoronata	0	0	0	1	0	1	-	0	1	1	0	0
Thismia okhaensis	0	0	0	1	0	0	-	0	1	1	1	1
Thismia pallida	0	0	0	0	-	1	-	1	1	1	1	1
Thismia panamensis	6	1	0	0	-	1	-	0	1	0	0	0
Thismia puberula	0	0	0	1	1	0	-	0	1	1	1	1
Thismia rodwayi	0	0	0	1	0	1	-	0	1	1	1	1
Thismia taiwanensis	0	0	0	2	-	1	-	1	1	1	0	0
Thismia tentaculata	0	0	0	0	-	1	-	0	1	1	1	1
Thismia thaithongiana	0	0	0	1	0	1	-	1	1	1	0	0
Thismia viridistriata	1	0	0	1	0	1	1	-	1	1	1	1
Afrothismia amietii	4	1	0	0	-	0	-	0	1	0	0	0
Afrothismia foertheriana	4	1	0	0	-	1	-	1	1	0	0	0
Afrothismia hydra	4	1	0	0	-	1	-	1	1	0	0	0
Afrothismia korupensis	4	1	0	0	-	1	-	1	1	0	0	0
Afrothismia kupensis	4	1	0	0	-	0	-	0	1	0	0	0
Afrothismia winkleri	4	1	0	0	-	1	-	1	1	0	0	0
Burmannia latialata	3	0	?	0	-	0	-	0	0	0	0	0
Dioscorea bulbifera	6	0	-	0	-	0	-	0	1	0	0	0
Haplothismia exannulata	2	0	0	0	-	0	-	0	1	0	0	0
Oxygyne shinzatoi	0	0	0	0	-	1	-	1	0	0	0	0
Tacca palmatifida	6	0	-	0	-	0	-	0	1	0	0	0
Tiputinia foetida	5	0	1	0	-	0	-	0	1	0	1	0

APPENDIX 3. Characters and character states used in ancestral state reconstruction.

Characters (and states) were as follows:

1. Underground part: creeping vermiform roots (0); coralliform roots (1); tuberous roots (2); filiform roots (3); short rhizome bearing clumps of small root tubercles (4); vertical cylindric sympodially branched rhizome (5); tuber (6).
2. Flower symmetry: actinomorphy (0); zygomorphy (1).
3. Transverse bars inside the hypanthium: absent (0); present (1).
4. Structure of inner perianth whorl: tepals free (0); tepals fused into mitre (1); tepals overlap forming a loose dome (2).
5. Foveae on mitre surface: absent (0); present (1). Species without a mitre are coded '-'.
6. Appendages of inner tepals: absent or < 1.5 mm long (0); present, > 1.5 mm long (1).
7. Mitre appendages arising from a central point: free from each other (0); fused into a column (1). Species without such appendages are coded '-'.
8. Appendages of outer tepals: absent (0); present (1). Species without outer tepals are coded '-'.
9. Stamen number: 3, opposite inner tepals (0); 6 (1).
10. Stamen connectives: free (0); postgenitally fused into a stamen tube (1).
11. Interstaminal glands: absent (0); present (1).
12. Wing-like appendage of a connective: absent (0); present (1).

SUPPORTING INFORMATION

Additional Supporting Information may be found in the online version of this article at the publisher's web-site:

Supplementary File S1. Mesquite Nexus file with morphological matrix and maximum likelihood ancestral state reconstruction.

Supplementary File S2. Supporting table and figures: table with BLAST results and accession numbers of sequences resulting from contamination. MrBayes and RAxML trees built from alignments of ITS, 18S, *atp1*, 18S+*atp1* and 18S+ITS matrices. Maximum likelihood ancestral state reconstructions in Mesquite: Flower symmetry; Mitre appendages arising from a central point; Stamen number; Stamen connectives.